This article has been accepted for publication in IEEE Internet of Things Journal. This is the author's version which has not been fully edited and content may change prior to final publication. Citation information: DOI 10.1109/JIOT.2022.3168658

Enhanced Modulation for Multi-Users Molecular Communication in Internet of Nano Things

Keyvan Aghababaiyan, *Student Member, IEEE*, Hamed Kebriaei, *Senior Member, IEEE*, Vahid Shah-Mansouri, *Member, IEEE*, Behrouz Maham, *Senior Member, IEEE*, and Dusit Niyato, *Fellow, IEEE*

***Abstract*—The novel concept of Internet of Nano Things (IoNT) brings even larger groups of nano-machines collaborating to achieve more complex tasks in the military, medical, and security fields. Moreover, Internet of Bio-Nano Things (IoBNT) is an emerging technology defining the seamless connection of nano-machines and biological entities with each other where they can access the traditional wireless communication networks to provide novel IoT applications such as health monitoring, health-care, and targeted therapy. The exchange of information between biological cells is based on the synthesis, transformation, emission, propagation, and reception of molecules. This information exchange is recently classified in telecommunications as molecular communication which is a biologically-inspired technique to communicate in very small dimension networks. In nano-networks, high number of nano-things will operate in the same medium and they interfere with each other. Multi-user interference will create significant limits. Hence, we introduce to use the direction of releasing molecules as a new property to convey information. Releasing the molecules to the specific directions enhances the performance of molecular communication systems due to multi-users interference mitigation. Hence, adjacent transmitters can convey information in different directions, simultaneously. Then, we propose the binary direction shift keying (BDSK) modulation scheme where the transmitter pumps molecules in two different directions. Next, we obtain the error probability and achievable bit rate of BDSK modulation. Finally, we evaluate the performance of BDSK modulation by numerical results. The result of this paper can be useful for molecular communication relay systems where relay nodes convey information to the different destinations.**

***Index Terms*— Internet of Nano Things, molecular communication, binary direction shift keying, achievable rate.**

I. Introduction

Recently, the concept of Internet of Things (IoT) [2] has been revised in light of novel research advances made in the field of nano-technology and communication engineering, which enable the development of nano-networks. The novel concept of Internet of Nano Things (IoNT) brings even larger groups of nano-machines collaborating to achieve more complex tasks [3], [4]. They can perform complex tasks such as health monitoring, environment monitoring and nano-medicine via cooperation and sharing information [5]. Various novel works aimed at the implementation of nano-technologies, especially biological nano-sensors to help in various disease diagnosis and treatment, forming the Internet of Bio-Nano Things (IoBNT) [4], [6]. To enable the IoBNT and its groundbreaking applications, such as continuous health monitoring and smart drug delivery, it is imperative to devise artificial communication techniques at nano-scale and bio-cyber interfaces to connect bio-nano-things with the macro-scale networks.

Information transmission between a pair of transmitter and receiver has been a challenge over decades. Exploiting electro-magnetic communication methods is the conventional solution. However, in very small dimensions such as nano-networks, these methods are inapplicable. Molecular communication is a biologically-inspired technique to communicate in very small dimension networks. Based on the IEEE P1906.1 definition, nano-networking is referred to as communication between two nano-scale components where at least one of them is controlled by humans. Molecular communication systems have numerous advantages such as energy efficient propagation [7], reliable propagation in challenging environments [8], [9], and information storage capacity [10]. In spite of these advantages, their performance has significant drawbacks such as high latency, low capacity, and sensitivity to environmental parameters [11].

Different molecular communication systems were introduced in the literature. Pheromone signaling, calcium signaling, and diffusion-based molecular communication are examples of proposed molecular communication systems [5]. Among them, diffusion-based molecular communication is the most simple, and energy-efficient communication system which does not need any infrastructure. Many different modulation schemes for diffusion-based molecular communication systems were proposed in the literature based on specific properties of the molecules.

- *Concentration of molecules:* Concentration Shift Keying (CSK) scheme was proposed in [12] where information was encoded in the concentration of released particles. When the concentration of released molecules is very low, the number of molecules can be exploited instead of the concentration of particles.
- *Type of molecules:* the information is encoded in the type of the released molecules. For example, in Molecular Shift Keying (MoSK) [12], two different types of molecules were employed to encode one bit of information. In addition, complex structures such as the DNA can be used to encode more information.
- *Structure of molecules:* the information is encoded as the ratio of molecules in the structure of the released particles. Isomer-based Ratio Shift Keying (IRSK) [13], Isomer-based Concentration Shift Keying (ICSK), and Isomer-based Molecule Shift Keying (IMoSK) [14] schemes are examples of this category.
- *Time of Release:* the massage is encoded in the releasing time of molecules. One example of timing based schemes

This research is supported, in part, by the programme DesCartes and is supported by the National Research Foundation, Prime Minister's Office, Singapore under its Campus for Research Excellence and Technological Enterprise (CREATE) programme, Alibaba Group through Alibaba Innovative Research (AIR) Program and Alibaba-NTU Singapore Joint Research Institute (JRI), the National Research Foundation, Singapore under the AI Singapore Programme (AISG) (AISG2-RP-2020-019), and Singapore Ministry of Education (MOE) Tier 1 (RG16/20). Corresponding author: Hamed Kebriaei.

Keyvan Aghababaiyan, Hamed Kebriaei, and Vahid Shah-Mansouri are with the School of Electrical and Computer Engineering, College of Engineering, University of Tehran, Tehran 14395-515, Iran. H. Kebriaei is also with the School of Computer Science, Institute for Research in Fundamental Sciences (IPM), P.O. Box 19395-5746, Tehran, Iran. His work was in part supported by a grant from the Institute for Research in Fundamental Sciences (IPM) under grant number: CS 1400-4-451. Behrouz Maham is with the Department of Electrical and Computer Engineering, School of Engineering, Nazarbayev University, Nur-Sultan, Kazakhstan, and Dusit Niyato is with the School of Computer Science and Engineering, Nanyang Technological University, Singapore 639798. Emails: aghababaiyan@ut.ac.ir, kebriaei@ut.ac.ir, vmansouri@ut.ac.ir, behrouz.maham@nu.edu.kz, dniyato@ntu.edu.sg.

A part of this work has been published in 2020 IEEE International Conference on Communications (ICC 2020), under the title of "Direction Shift Keying Modulation for Molecular Communication" [1].

This article has been accepted for publication in IEEE Internet of Things Journal. This is the author's version which has not been fully edited and content may change prior to final publication. Citation information: DOI 10.1109/JIOT.2022.3168658

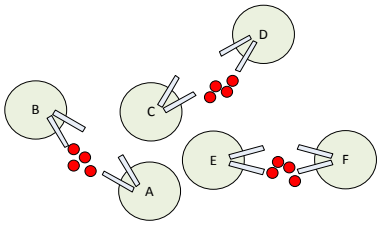

Fig. 1: Multi-users interference in a molecular communication network

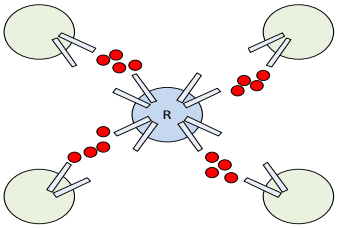

Fig. 2: A simple molecular communication relay-based network

is Pulse Position Modulation (PPM) [15]. This modulation is similar to PPM in optical communication where a large number of molecules are released by the transmitter at a specific time to generate a pulse. In this case, the exact time synchronization between the transmitter and receiver is required, which is beyond the capabilities of nano-machines.

Therefore, in the mentioned modulation schemes, information is encoded in terms of the concentration, type, ratio, and releasing time of molecules.

In nano-networks, high number of nano things will operate in the same medium and they interfere with each other when they use one type of molecule and work based on the concentration of molecules. Multi-user interference will create significant limits in the communication network. The first solution to tackle the interference problem is utilizing different types of molecules or different structures of molecules for different transmitter-receiver pairs. This strategy is impractical in the large networks since there are many nano-things working at the same volume. On the other hand, using the releasing time for information transmission needs the exact time synchronization between the transmitter and receiver which is beyond the capabilities of nano-machines. Hence, in this paper, we suggest the direction of releasing molecules as a new property of molecules to convey information in molecular communication systems which is beneficial for multi-users interference mitigation in the large molecular communication networks. For example, in Fig. 1, there are three transmitter-receiver pairs. When one of the transmitters, i.e., nodes A, C, and E, releases molecules in all of directions, the other nodes cannot convey information due to multi-users interference. However, when the transmitters release molecules to the specific directions, they can release molecules without any interference, simultaneously. Hence, nodes A, C, and E, can convey information to nodes B, D, and F, respectively.

One of the challenges in molecular communication is that the propagation time increases with the square of the distance. If an intended receiver is far away from the transmitter, then using a single transmitter may be impractical. One approach in conventional wireless communications that can be adopted for molecular communication is the use of intermediate transceivers acting as relays to aid the communication with distant receivers. Such relays can potentially improve the reliability and performance of a communication link [16]. Hence, relay-assisted diffusion-based molecular communication systems can improve the error probability of data transmission through reducing the distance between transmitter-receiver pairs. Moreover, as shown in Fig. 2, the relay nodes can convey information to the different destinations, simultaneously by releasing molecules in the specific directions. If we do not use different directions, the relay node (R) needs more time to transmit information to the different receivers. If the relay node releases molecules to all of directions, it needs four time slots to transmit information to different receivers in the assumed scenario. Hence, releasing the molecules to the specific directions enhances the performance of diffusion-based molecular communication relay systems due to multi-users interference mitigation.

The main contributions of this paper can be summarized as follows:

- We introduce the direction of releasing of molecules as a new degree of freedom to convey information with the goal of interference mitigation for diffusion-based molecular communication applications in IoNT and IoBNT. We derive the concentration of molecules in the 3-D diffusion environment when the transmitter employs different directions to transmit information. To the best of our knowledge, this is the first analytical work in the literature to analyze the molecular communication systems when the transmitter releases molecules in a specific direction.
- Then, we propose BDSK modulation as a simple scenario where the transmitter nano-machine uses two different directions to release molecules. We present the optimum decision rule for the receiver through counting the number of absorbed molecules by different sectors of the receiver. The presented analysis for BDSK modulation can be generalized for more complex modulations through changing the definition of sectors on the receiver surface and the number of directions of releasing molecules.
- Next, we obtain the error probability and achievable rate of BDSK modulation when there exist inter-symbol interference, inter-link interference molecules, and the signal dependent noise. Due to the acceptable error probability and achievable rate, releasing molecules in the specific directions can be useful for molecular communication systems where different nodes can release molecules at the same time to convey information to the different destinations.
- Finally, we analyze the channel impulse response in different simulation scenarios and use particle-based simulations to verify analytical results. Moreover, we study the error probability and achievable rate of BDSK modulation for different values of symbol duration and different distances between the receiver and transmitter through employing numerical results.

This paper is organized as follows. In Section II, we present the works related to the molecular communication. In Section III, we present our system model. Then, in Section IV, we derive the concentration of molecules in the 3-D diffusion environment when the transmitter releases molecules in a specific direction. We propose BDSK modulation scheme in Section V. Next, we obtain the error probability and achievable rate of BDSK modulation in this section. We present numerical results in Section VI. Finally, we conclude this paper in Section VII.

This article has been accepted for publication in IEEE Internet of Things Journal. This is the author's version which has not been fully edited and content may change prior to final publication. Citation information: DOI 10.1109/JIOT.2022.3168658

II. Related Works

Diffusion-based molecular communication was extensively investigated from different facets over the last decade. Some research works proposed different modulation schemes for diffusion-based molecular communication systems based on specific properties of the molecules. CSK scheme was proposed in [12] where information was encoded in the concentration of released particles. In MoSK [12], different types of molecules were employed to encode information. In IRSK [13], ICSK, and IMoSK [14] schemes, the information is encoded as the ratio of molecules in the structure of the released particles. In PPM [15], the massage is encoded in the releasing time of molecules. Moreover, some modulation schemes have been proposed which employ more than one of these preceding techniques [17], [18]. The authors of [17] proposed Molecular Concentration Shift Keying (MoCSK). MoCSK brings MoSK idea to the CSK. The study in [18] combined time-based and molecule type-based modulation schemes. In [19], molecular type permutation shift keying modulation was proposed for multiple-input multiple output (MIMO) molecular communication systems to improve the bit error probability performance.

Some papers in the existing literature proposed theoretical models for molecular communication applications and the implementation of molecular communication systems such as communication through calcium ion exchange in [20]. The authors of [21] introduced a molecular motor communication system. The authors of [22] studied a molecular communication system exploited for future health-care applications. An autonomous molecular propagation system was proposed in [23]. The authors of [24] designed a molecular communication game in which nano-machines choose to cooperate or confront. They investigated the performances of anarchic and cooperative transmitters in Internet of Molecular Things (IoMT). The authors of [25] studied the theoretical limits on multi-users molecular communication in IoBNT. The authors of [26] proposed a resource allocation scheme for multi-users molecular communication systems oriented to the Internet of Medical Things (IoMT).

Some other papers in the literature developed information theoretical models for molecular communication channels and analyzed the capacity of molecular communication channels. The capacity bounds of molecular communication channel with considering a Brownian motion model without drift were derived in [27]. In [28], the capacity of molecular communication channel was obtained by simulation with adding a positive drift to the Brownian motion. In [29], an amplify-and-forward molecular communication relay scheme for optimizing channel capacity was proposed. The authors of [29] evaluated the performance of different detection methods and they obtained the optimal signal detection threshold when the MAP detection method was used. The authors of [30] proposed a scheme to detect relative location of the silent absorbing target in a three-node molecular communication system including a point source transmitter, a passive receiver and a silent absorbing target and then analyzed the performance of this scheme. The authors of [31] and [32] derived the mutual information for simple on-off keying models. The authors of [33] analyzed the performance of depleted molecule shift keying (D-MoSK) modulation. The capacity of multiple-input multiple output (MIMO) molecular communication systems was derived in [34]. The mutual information of multi-users molecular communication channels was analyzed in [35].

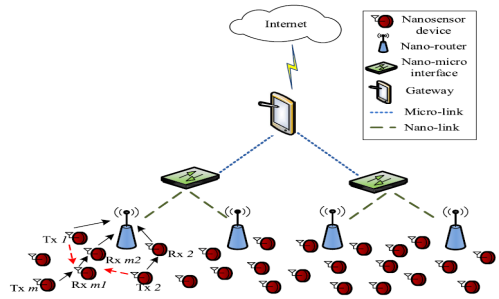

Fig. 3: Network architecture for the IoNT and IoBNT [36]

III. System Model

In this section, first we present the network architecture of IoNT and IoBNT. Then, we introduce the assumed system model for molecular communication between two nano-sensors or nano-machines in IoBNT.

A. Network Architecture for the IoNT and IoBNT

The nano-machines, nano-biosensors and engineered bacteria are connected with each other in IoNT and IoBNT, respectively, which can access the traditional wireless communication networks to provide novel IoT applications such as environment monitoring, health monitoring, health-care, and targeted therapy. Fig. 3 shows a schematic of network architecture for the IoNT and IoBNT. Biological nano-sensor nodes inside the human body and nano-machines are nano-nodes of these networks. They transmit their information to nano-routers. Nano-routers have larger computational resources than nano-nodes and they are suitable for aggregating information. Then, nano-micro interface devices aggregate the information coming from nano-routers. The transmitted messages from the nano-micro interface are received by the gateway. The gateway enables the remote control of the entire system over the Internet. The gateway can be an advanced smart-phone.

The development of IoNT and IoBNT lays the foundation for future research and development of nano-scale Internet and nano-communication technology. Molecular communication is a bio-inspired communication technology to enable communication in a nano-micro scale, which has stimulated a great deal of interest in both academic and medical domains.

B. Molecular Communication Model

The molecular communication system under consideration in this paper includes a pair of transmitter and receiver nano-machines in a 3-D environment which is extended to infinity in all dimensions. Fig. 4 represents the schematic of this system. This communication system is represented by a spherical coordinate space. The center of the receiver is located at the distance r_0 from the center of the transmitter. The radius of the transmitter and receiver are denoted as r_{tx} and r_{rx}, respectively, where $r_{\text{tx}} = r_{\text{rx}}$ similar to the assumed scenarios in [37] and [38]. In this system, the pair of transmitter and receiver are fixed and they do not rotate during the data transmission process. We consider that releasing points are uniformly distributed with respect to the azimuth angle on the surface of the transmitter and receiver similar to the considered receivers in [39] and [40]. The transmitter emits only one type of molecule, e.g., pheromones or hormones for information transmission. We consider a spherical transmitter with reflective boundary and a spherical receiver with fully absorbing boundaries [41], [42]. The receiver absorbs

This article has been accepted for publication in IEEE Internet of Things Journal. This is the author's version which has not been fully edited and content may change prior to final publication. Citation information: DOI 10.1109/JIOT.2022.3168658

molecules to detect the information bit. This means that each molecule is absorbed and eliminated from the diffusion environment when it collides with the surface of receiver. Thus, the distance between each point in the diffusion environment and the closest point on the surface of the receiver along the X axis is denoted by r. We hypothesize that the receiver nano-machine is sensitive to a specific type of information molecule and it is capable of counting the number of absorbed molecules in every time interval to decode information [43]. Furthermore, we assume that the transmitter and receiver are synchronous as in [44]. Therefore, time is divided into equal duration slots easily in which a single symbol is sent. These time slots are called symbol durations. In addition, we suppose that the diffusion environment is fully filled with a fluid with a constant diffusion coefficient, i.e., D. In this environment, molecules diffuse independently. This means, the concentration of molecules is sufficiently low as we can ignore the collisions between them [45].

In the considered diffusion-based molecular communication system, molecules have a random motion which is called Brownian motion [45]. Based on the described system model, in this paper, we propose a new modulation scheme where the transmitter nano-machine in Fig. 4 pumps molecules in the specific directions to encode information. In fact, an important class of transport mechanisms are molecule pumps. Based on the source of energy driving the molecule pumps, two main types of molecule pumps are light driven pumps and adenosine triphosphate (ATP) driven pumps [46]. Since light introduces a high degree of spatial and temporal flexibility and control, light driven pumps are highly attractive for implementing the modulation process in nano-machines.

Pumping molecules in the specific directions has many advantages in comparison to other modulation schemes. This strategy works by using one type of molecules similar to the CSK and timing-based schemes, while MoSK and Isomer-based modulations need more types of molecules. Using different molecule types complicates the hardware structure at both the transmitter and the receiver, exponentially. Moreover, the proposed scheme needs no synchronization unlike the timing-based modulation schemes. In addition, the proposed scheme provides higher data rate in comparison to the CSK and timing-based schemes since its sensitivity to the inter symbol interference molecules is lower than other schemes, and thus, it can work with using shorter symbol durations. Hence, the main advantage of the proposed scheme is reducing the effect of interfering molecules due to pumping the molecules to a specific direction [46], which enhances the performance of diffusion-based molecular communication systems. For example, in Fig. 4, the transmitter employs directions φ_1 and φ_2 to distinguish between bits 0 and 1. The released molecules in the directions of φ_1 and φ_2 are uniformly distributed with respect to the azimuth angle, i.e., θ, in the interval of $\theta \in [0, \pi]$. It is worth mentioning that the proposed scheme is practical in the scenarios where the sizes of transmitter and receiver are comparable with their distance such as neuro-synaptic communication [47] where neuro-transmitter molecules are used to convey information between neurons through synapses [48], [49]. In the next section, we derive the concentration of molecules in the diffusion environment when the transmitter releases molecules in a specific direction.

IV. Concentration of Molecules in Diffusion Environment

In this section, we derive the concentration of molecules in the 3-D diffusion environment when the transmitter employs DSK scheme to transmit information. The diffusion process in a 3-D environment can be described by Fick's second law [50] as

$$\frac{\partial \Upsilon(r,\theta,\varphi,t|R(\varphi_1),\varphi_1)}{\partial t} = D\,\nabla^2 \Upsilon(r,\theta,\varphi,t|R(\varphi_1),\varphi_1), \quad (1)$$

where ∇^2 is the Laplacian operator, $R(\varphi) = r_0\cos(\varphi) - \sqrt{r_{tx}^2 - r_0^2\sin^2(\varphi)}$ is the distance between the boundary of the transmitter at φ and the center of receiver, and $\Upsilon(r,\theta,\varphi,t|R(\varphi_1),\varphi_1)$ shows the concentration of molecules at time t and distance r when they are released from a source at the initial distance $R(\varphi_1)$ in the direction of $\varphi = \varphi_1$, and D is the diffusion coefficient which depends on the viscosity of the fluid and temperature. In this paper, unlike the previous works that only considered the effect of radius on the concentration of molecules, we investigate the variation of the concentration of molecules with respect to the azimuth and elevation angles, i.e., θ and φ. Hence, in this situation, solving the Fick's second law problem is different since the Laplacian operator and the initial conditions are functions of the radius, azimuth and elevation angles, simultaneously. To solve the Fick's 3-D diffusion problem, we need to specify the initial and boundary conditions. Hence, we define the initial condition as

$$\Upsilon(r,\theta,\varphi,t\to 0|R(\varphi_1),\varphi_1) = N\delta(r - R(\varphi_1))\delta(\varphi-\varphi_1), \theta \in [0,\pi], \quad (2)$$

where $\delta(.)$ is the Dirac delta function and N is the number of released molecules. Since molecules are eliminated when they are very far away from the receiver, we consider the first boundary condition as [50]

$$\lim_{r\to\infty} \Upsilon\,(r,\theta,\varphi,t|R(\varphi_1),\varphi_1) = 0. \quad (3)$$

Since we have a receiver with fully absorbing boundaries, the second boundary condition can be defined as [50]

$$\Upsilon(r_{\rm rx},\theta,\varphi,t|R(\varphi_1),\varphi_1) = 0. \quad (4)$$

In addition, we have a transmitter with reflective boundary, and thus, we define the third boundary condition [51] as

$$\frac{\delta\Upsilon\,(r,\theta,\varphi,t|R(\varphi_1),\varphi_1)}{\delta r}|_{r=R(\varphi)} = 0. \quad (5)$$

This boundary condition shows that the transmitter reflects all of molecules to the diffusion environment when they collide the

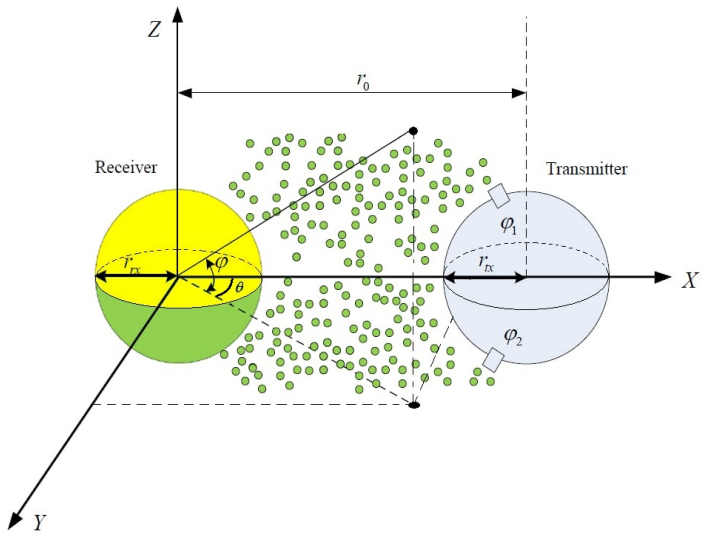

Fig. 4: System model for communication between two nano-machines

This article has been accepted for publication in IEEE Internet of Things Journal. This is the author's version which has not been fully edited and content may change prior to final publication. Citation information: DOI 10.1109/JIOT.2022.3168658

surface of transmitter. In spherical coordinates, Fick's second law can be rewritten as

$$\frac{1}{D}\frac{\partial \Upsilon}{\partial t} = \frac{1}{r^2}\frac{\partial}{\partial r}\left(r^2\frac{\partial \Upsilon}{\partial r}\right) + \frac{1}{r^2\sin(\theta)}\frac{\partial}{\partial \theta}\left(\sin(\theta)\frac{\partial \Upsilon}{\partial \theta}\right) + \frac{1}{r^2\sin(\theta)^2}\frac{\partial^2 \Upsilon}{\partial \varphi^2}, \quad (6)$$

where the solution of this equation, i.e., $\Upsilon(r,\theta,\varphi,t|R(\varphi_1),\varphi_1)$, is a general function of r, θ, φ and t. Using the separation of variables technique, $\Upsilon(r,\theta,\varphi,t|R(\varphi_1),\varphi_1)$ can be written as

$$\Upsilon(r,\theta,\varphi,t|R(\varphi_1),\varphi_1) = \lambda(r,t|R(\varphi_1),\varphi_1)\beta(\theta,t|R(\varphi_1),\varphi_1)\gamma(\varphi,t|R(\varphi_1),\varphi_1), \quad (7)$$

where $\lambda(r,t|R(\varphi_1),\varphi_1)$ is independent of θ and φ, $\beta(\theta,t|R(\varphi_1),\varphi_1)$ is independent of r and φ, $\gamma(\varphi,t|R(\varphi_1),\varphi_1)$ is independent of r and θ. By inserting the expression in (7) into (6), we have

$$\frac{\partial \Upsilon(r,\theta,\varphi,t|R(\varphi_1),\varphi_1)}{\partial t} = D\frac{\beta(\theta,t|R(\varphi_1),\varphi_1)\gamma(\varphi,t|R(\varphi_1),\varphi_1)}{r}\frac{\partial^2}{\partial r^2}\left(r\lambda(r,t|R(\varphi_1),\varphi_1)\right) + D\frac{\lambda(r,t|R(\varphi_1),\varphi_1)\gamma(\varphi,t|R(\varphi_1),\varphi_1)}{r^2\sin(\theta)} \times \frac{\delta}{\delta\theta}\left(\sin(\theta)\frac{\delta\beta(\theta,t|R(\varphi_1),\varphi_1)}{\delta\theta}\right) + D\frac{\lambda(r,t|R(\varphi_1),\varphi_1)\beta(\theta,t|R(\varphi_1),\varphi_1)}{r^2\sin^2(\theta)}\frac{\partial^2\gamma(\varphi,t|R(\varphi_1),\varphi_1)}{\partial\varphi^2}. \quad (8)$$

Moreover, using (7), we can write

$$\frac{\partial \Upsilon(r,\varphi,t|R(\varphi_1),\varphi_1)}{\partial t} = \gamma(\varphi,t|R(\varphi_1),\varphi_1)\beta(\theta,t|R(\varphi_1),\varphi_1)\frac{\partial\lambda(r,t|R(\varphi_1),\varphi_1)}{\partial t} + \lambda(r,t|R(\varphi_1),\varphi_1)\gamma(\varphi,t|R(\varphi_1),\varphi_1)\frac{\partial\beta(\theta,t|R(\varphi_1),\varphi_1)}{\partial t} + \lambda(r,t|R(\varphi_1),\varphi_1)\beta(\theta,t|R(\varphi_1),\varphi_1)\frac{\partial\gamma(\varphi,t|R(\varphi_1),\varphi_1)}{\partial t}. \quad (9)$$

Plugging the expression in (9) into (8) and comparing two sides of the resulted equation, we can divide Fick's second law problem into the following problems as

$$\frac{\partial\lambda(r,t|R(\varphi_1),\varphi_1)}{\partial t} = \frac{D}{r}\frac{\partial^2}{\partial r^2}\left(r\,\lambda(r,t|R(\varphi_1),\varphi_1)\right), \quad (10)$$

$$\frac{\partial\beta(\theta,t|R(\varphi_1),\varphi_1)}{\partial t} = \frac{D}{r^2\sin(\theta)}\frac{\delta}{\delta\theta}\left(\sin(\theta)\frac{\delta\beta(\theta,t|R(\varphi_1),\varphi_1)}{\delta\theta}\right)|_{r=cte}, \quad (11)$$

$$\frac{\partial\gamma(\varphi,t|R(\varphi_1),\varphi_1)}{\partial t} = \frac{D}{r^2\sin^2\theta}\frac{\partial^2}{\partial\varphi^2}\gamma(\varphi,t|R(\varphi_1),\varphi_1)|_{r=cte}. \quad (12)$$

The first problem stated in (10) is independent of θ and φ, the second problem in (11) is independent of φ, and it is considered for a constant r; and the third one is considered for a constant r and θ. Using the separation of variables technique for the expression in (2), initial conditions can be partitioned as

$$\lambda(r,t\to 0|R(\varphi_1),\varphi_1) = N\delta(r-R(\varphi_1)), \quad (13)$$

$$\beta(\theta,t\to 0|R(\varphi_1),\varphi_1) = 1, \quad (14)$$

$$\gamma(\varphi,t\to 0|R(\varphi_1),\varphi_1) = \delta(\varphi-\varphi_1). \quad (15)$$

The initial conditions in (13), (14), (15) are employed for solving the problems in (10), (11), and (12), respectively.

Proposition 1. *The solution of the problem described in (10) using the initial condition in (13), is obtained as*

$$\lambda(r,t|R(\varphi_1),\varphi_1) = \frac{N}{r\sqrt{4\pi Dt}}[\exp(-\frac{(r-R(\varphi_1))^2}{4Dt}) - \exp(-\frac{R(\varphi_1)^2}{4Dt})\exp(\frac{2r_{rx}R(\varphi_1)}{4Dt})\exp(-\frac{r^2}{4Dt})] + \frac{N}{r\sqrt{4\pi Dt}}[\exp(-\frac{(r-R(\varphi_1))^2}{4Dt}) - \frac{2Dt+R(\varphi)^2-R(\varphi)R(\varphi_1)}{R(\varphi)^2+2Dt} \times \exp\left(-\frac{R(\varphi_1)^2-2R(\varphi)R(\varphi_1)}{4Dt}\right)\exp(-\frac{r^2}{4Dt})]. \quad (16)$$

Proof: The proof is given in Appendix A.

Proposition 2. *The solution of the problem described in (11) with using the initial condition in (14), is obtained as*

$$\beta(\theta,t|R(\varphi_1),\varphi_1) = 1. \quad (17)$$

Proof: The proof is given in Appendix B.

Proposition 3. *The solution of the problem described in (12) with using the initial condition in (15), is obtained as*

$$\gamma(\varphi,t|R(\varphi_1),\varphi_1) = \frac{r\sin\theta}{\sqrt{4\pi Dt}}\exp\left(-\frac{r^2\sin^2\theta(\varphi-\varphi_1)^2}{4tD}\right). \quad (18)$$

Proof: The proof is given in Appendix C.

Finally, inserting the results of Proposition 1, 2, and 3, into (7), the molecules concentration in the diffusion environment, i.e., $\Upsilon(r,\theta,\varphi,t|R(\varphi_1),\varphi_1)$ can be derived.

V. BDSK MODULATION FOR COMMUNICATION BETWEEN TWO NANO-MACHINES

In this paper, we propose BDSK modulation which conveys information according to the direction of releasing molecules by transmitter. Generally, in different modulations, the number of possible code words with length of k is $l_k = l^k$ when the transmission alphabet contains l different symbols. For BDSK modulation, we have $l = 2$, and thus, the alphabet includes two symbols, i.e., $\{0,1\}$. It is worth noting that the presented analysis for $l = 2$ can be generalized to any values of l, and the only differences are the definition of sectors on the receiver surface and the directions of releasing molecules. Fig. 4 shows the schematic of using BDSK modulation in a scenario where we hypothesize that the transmitter releases molecules in $\varphi = \varphi_1$ direction to convey bit 1 and releases molecules in $\varphi = \varphi_2$ direction to convey bit 0. On the receiver side, we consider a 3-D spherical receiver with fully absorbing boundaries. The receiver is capable of distinguishing the absorbed molecules by different spherical sectors which are distinguished in terms of azimuth angle. The first sector, i.e., Ω_{r1}, is defined in $\varphi_{\text{th}} \le \varphi \le \frac{\pi}{2}$ range and the second one, i.e., Ω_{r2}, is defined in $-\frac{\pi}{2} \le \varphi \le \varphi_{\text{th}}$ range, where φ_{th} is the boundary between the defined sectors on the receiver surface. The receiver counts the number of absorbed molecules by each sector in every symbol duration to detect information. It detects bit 1, when the number of absorbed molecules by the first sector is more than that of the second one. On the other hand, the receiver detects bit 0 when the number of absorbed molecules by the second sector is more than that of

This article has been accepted for publication in IEEE Internet of Things Journal. This is the author's version which has not been fully edited and content may change prior to final publication. Citation information: DOI 10.1109/JIOT.2022.3168658

the first sector. We described the concentration of molecules in the diffusion environment in (7). According to the expression in (7), the hitting rate of molecules to the first sector of receiver, i.e., Ω_{r1} is defined as

$$n_{\text{hit}}(\Omega_{r1}, t|R(\varphi_1), \varphi_1) = \int_{\varphi_{\text{th}}}^{\frac{\pi}{2}} \int_0^{\pi} D \frac{\partial \Upsilon(r, \theta, \varphi, t|R(\varphi_1), \varphi_1)}{\partial r} r^2 \sin\theta d\theta d\varphi|_{r=r_{\text{rx}}}, \quad (19)$$

where r_{rx} is the radius of receiver. Similarly, the hitting rate of molecules to the second sector, i.e., Ω_{r2} is obtained as

$$n_{\text{hit}}(\Omega_{r2}, t|R(\varphi_1), \varphi_2) = \int_{-\frac{\pi}{2}}^{\varphi_{\text{th}}} \int_0^{\pi} D \frac{\partial \Upsilon(r, \theta, \varphi, t|R(\varphi_1), \varphi_2)}{\partial r} r^2 \sin\theta d\theta d\varphi|_{r=r_{\text{rx}}}. \quad (20)$$

At the end of each symbol duration, some of molecules remain in the diffusion medium and affect the detection process of next symbols. This phenomenon is denoted as Inter Symbol Interference (ISI). In this paper, we consider a memory for the channel denoted by L as the number of former symbol durations which affect the detection process. Moreover, in the diffusion process, the released molecules towards a special sector can affect the other sector. These molecules are denoted as Inter Link Interference (ILI). According to the expression in (7), the hitting rate of ILI molecules to the first sector, i.e., the molecules which are released in the direction of $\varphi = \varphi_2$, while they are absorbed by the first sector of receiver, is obtained as follows:

$$n'_{\text{hit}}(\Omega_{r1}, t|R(\varphi_1), \varphi_2) = \int_{\varphi_{\text{th}}}^{\frac{\pi}{2}} \int_0^{\pi} D \frac{\partial \Upsilon(r, \theta, \varphi, t|R(\varphi_1), \varphi_2)}{\partial r} r^2 \sin\theta d\theta d\varphi|_{r=r_{\text{rx}}}, \quad (21)$$

and the hitting rate of ILI molecules to the second sector, i.e., the molecules which are released in the direction of $\varphi = \varphi_1$, while they are absorbed by the second sector of receiver, is derived as

$$n'_{\text{hit}}(\Omega_{r2}, t|R(\varphi_1), \varphi_1) = \int_{-\frac{\pi}{2}}^{\varphi_{\text{th}}} \int_0^{\pi} D \frac{\partial \Upsilon(r, \theta, \varphi, t|R(\varphi_1), \varphi_1)}{\partial r} r^2 \sin\theta d\theta d\varphi|_{r=r_{\text{rx}}}. \quad (22)$$

A. Decision Regions

In the BDSK modulation, the optimum receiver partitions the output space into two regions to separate bits 1 and 0 according to the number of received molecules. The number of information molecules absorbed until time t by each spherical sector, i.e., $N_{\text{hit}}(\Omega_{ri}, t|R(\varphi_1), \varphi_i)$, for $i = 1, 2$ is obtained by integrating $n_{\text{hit}}(\Omega_{ri}, t|R(\varphi_1), \varphi_i)$ as

$$N_{\text{hit}}(\Omega_{ri}, t|R(\varphi_1), \varphi_i) = \int_0^t n_{\text{hit}}(\Omega_{ri}, t'|R(\varphi_1), \varphi_i) dt'. \quad (23)$$

In a similar way, the number of ILI molecules absorbed until time t by each spherical sector, i.e., $N'_{\text{hit}}(\Omega_{ri}, t|R(\varphi_1), \varphi_j)$ for $i \neq j$ is obtained by integrating $n'_{\text{hit}}(\Omega_{ri}, t|R(\varphi_1), \varphi_j)$ as

$$N'_{hit}(\Omega_{ri}, t|R(\varphi_1), \varphi_j) = \int_0^t n'_{hit}(\Omega_{ri}, t'|R(\varphi_1), \varphi_j) dt'. \quad (24)$$

By applying the Bayes criterion, the likelihood ratio for distinguishing bits 1 and 0 is defined as

$$\text{L}_{\varphi}(\varphi) = \frac{N_{\text{hit}}(\Omega_{rm}, T|R(\varphi_1), \varphi_m)}{N_{\text{hit}}(\Omega_{rm'}, T|R(\varphi_1), \varphi'_m)}. \quad (25)$$

For the binary decision, the region Ω_{rm} consists of the value of φ that $\text{L}_{\varphi}(\varphi) \geq 1$. Thus, the decision rule for the optimum detector according to the number of received molecules is described as

$$D_m = \{\varphi_m \in \left(0, +\frac{\pi}{2}\right) : N_{\text{hit}}(\Omega_{rm}, T|R(\varphi_1), \varphi_m) \geq N_{\text{hit}}(\Omega_{rm'}, T|R(\varphi_1), \varphi'_m), m \neq m'\}, \quad (26)$$

where T denotes the symbol duration of the considered communication system and D_m is the decision region of message m. This expression means the number of absorbed molecules by the Ω_{rm} region when the molecules are released in the direction of φ_m should be more than the number of absorbed molecules by the $\Omega_{rm'}$ region when the molecules are released in the direction of φ'_m, where $\varphi_m \in \left(0, +\frac{\pi}{2}\right)$.

B. Error Probability and Achievable Rate of BDSK Modulation

In this section, we evaluate the performance of BDSK modulation through analysis of the error probability. Moreover, we obtain the achievable rate of BDSK modulation to investigate its efficiency. The expected number of received information molecules by the first spherical sector of receiver at time t when the molecules are released at $t = iT$ is given by

$$h_{i1}(t) = N_{hit}(\Omega_{r1}, t|R(\varphi_1), \varphi_1) - N_{hit}(\Omega_{r1}, iT|R(\varphi_1), \varphi_1), \quad (27)$$

where T denotes the symbol duration. In addition, the expected number of ILI molecules which are received by the first spherical sector at time t when the information molecules are released at $t = iT$ by the second transmitter, is obtained as

$$h'_{i1}(t) = N'_{hit}(\Omega_{r1}, t|R(\varphi_1), \varphi_2) - N'_{hit}(\Omega_{r1}, iT|R(\varphi_1), \varphi_2). \quad (28)$$

In a similar way, the expected number of received information molecules by the second spherical sector at time t when the molecules are released at $t = iT$ is given by

$$h_{i2}(t) = N_{hit}(\Omega_{r2}, t|R(\varphi_1), \varphi_2) - N_{hit}(\Omega_{r2}, iT|R(\varphi_1), \varphi_2). \quad (29)$$

Furthermore, the expected number of ILI molecules which are received by the second spherical sector at time t when the information molecules are released at $t = iT$ by the first transmitter, is obtained as

$$h'_{i2}(t) = N'_{hit}(\Omega_{r2}, t|R(\varphi_1), \varphi_1) - N'_{hit}(\Omega_{r2}, iT|R(\varphi_1), \varphi_1). \quad (30)$$

We assume that $y_1(t)$ represents the number of molecules sensed by the first receiver at time t as

$$y_1(t) = \sum_{i=0}^{L} h_{i1}(t + iT)x_i + \sum_{i=0}^{L} h'_{i1}(t + iT)(1 - x_i) + n_1(t), \quad (31)$$

where x_i denotes the information bit transmitted in i-th symbol duration and L is the system memory. The expression in (31) can be rewritten as

$$y_1(t) = h_{01}(t)x_0 + \sum_{i=1}^{L} h_{i1}(t + iT)x_i + \sum_{i=0}^{L} h'_{i1}(t + iT)(1 - x_i) + n_1(t) = h_{01}(t)x_0 + I_1(t) + I'_1(t) + n_1(t), \quad (32)$$

where $h_{01}(t)x_0$ is the absorbed information molecules from the first transmitter in this symbol duration, $I_1(t)$ shows the ISI molecules from the last L symbol durations and $I'_1(t)$ represents the ILI molecules from the last $L + 1$ symbol durations, respectively. We hypothesize that the ISI and ILI molecules resulted from L former symbols have a comparable effect in confusing the signal detection. The $n_1(t)$ is a signal dependent noise sensed

This article has been accepted for publication in IEEE Internet of Things Journal. This is the author's version which has not been fully edited and content may change prior to final publication. Citation information: DOI 10.1109/JIOT.2022.3168658

TABLE I: Simulation parameters

Parameter	Symbol	Value
Radius of receiver	r_{rx}	$5\,\mu$m
Simulation Time Step	Δt	$10^{-3}s$
Number of Molecules	N	100
Initial velocity	V_0	$5\,\mu$m
Potential of strongest attractive point	ε	1
Minimum distance without interaction	σ	2.5 nm
Random acceleration	σ^{*^2}	$1\,\mu\text{m}^2$

by the first receiver. The noise component is assumed to follow a Gaussian distribution represented as $n_1(t) \sim N(\mu_{n1}(t), \sigma^2_{n1}(t))$, associated with $\mu_{n1}(t) = 0, \quad \sigma^2_{n1}(t) = \frac{h_{01}(t)x_0 + I_1(t)}{V_{RX1}}$, [52] where V_{RX1} is the volume of the first sector of the spherical receiver. When we have $\varphi_{\text{th}} = 0$, we conclude $V_{RX1} = \frac{2}{3}\pi r^3_{\text{rx}}$, where r_{rx} is the radius of the receiver nano-machine. Similarly, $y_2(t)$ represents the number of molecules sensed by the second receiver at time t as

$$y_2(t) = \sum_{i=0}^{L} h_{i2}(t + iT)\,(1 - x_i) + \sum_{i=0}^{L} h'_{i2}(t + iT)x_i + n_2(t), \tag{33}$$

where x_i denotes the information bit transmitted in i-th symbol duration. The expression in (33) can be rewritten as

$$\begin{aligned} y_2(t) &= h_{02}(t)\,(1 - x_0) + \sum_{i=1}^{L} h_{i2}(t + iT)\,(1 - x_i) \\ &\quad + \sum_{i=0}^{L} h'_{i2}(t + iT)x_i + n_2(t) \\ &= h_{02}(t)\,(1 - x_0) + I_2(t) + I'_2(t) + n_2(t), \end{aligned} \tag{34}$$

where $h_{02}(t)\,(1 - x_0)$ is the absorbed information molecules from the second transmitter in this symbol duration, $I_2(t)$ shows the ISI molecules from the last L symbol durations and $I'_2(t)$ depicts the ILI molecules from the last $L + 1$ symbol durations, respectively. The $n_2(t)$ is a signal dependent noise sensed by the second receiver. The noise component is considered as a Gaussian distribution represented as $n_2(t) \sim N(\mu_{n2}(t), \sigma^2_{n2}(t))$, associated with $\mu_{n2}(t) = 0, \quad \sigma^2_{n2}(t) = \frac{h_{02}(t)(1-x_0) + I_2(t)}{V_{RX2}}$, [52] where V_{RX2} is the volume of the second sector of spherical receiver nano-machine. When we have $\varphi_{\text{th}} = 0$, it is concluded that $V_{RX2} = \frac{2}{3}\pi r^3_{\text{rx}}$, where r_{rx} is the radius of the receiver nano-machine. According to the expressions in (32) and (34), the number of received molecules by the m-th sector of receiver at the end of i-th symbol duration is defined as $y^{iT}_m = y_m(iT)$. Thus, the error probability of the optimum receiver to detect the i-th symbol through employing the described decision rule in (23) is derived as

$$\begin{aligned} P_e &= P_r(x_i = 0)\, P_r(y^{iT}_2 \le y^{iT}_1 | x_i = 0) \\ &\quad + P_r(x_i = 1)\, P_r(y^{iT}_2 \ge y^{iT}_1 | x_i = 1). \end{aligned} \tag{35}$$

To analyze the achievable bit rate of the proposed scheme, we use the Shannon's classical channel capacity formula, i.e., $C = \underset{P(X)}{\text{Max}}\ I(X, Y)$. Since the diffusion-based molecular communication channel is not a memory less channel, we need to employ the general formulation for the mutual information rate as

$$I\,(X, Y) = \lim_{n\to\infty} \frac{1}{n} I\,(X_1, \ldots, X_n; Y_1, \ldots, Y_n)\,. \tag{36}$$

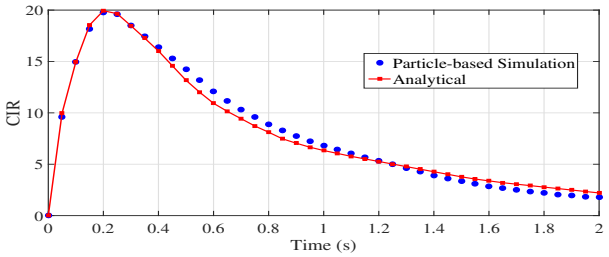

Fig. 5: Analytical and simulation results for the CIR, when $r_0 = 15\mu m$, $\varphi_1 = 0$ and $\theta = 45^o$.

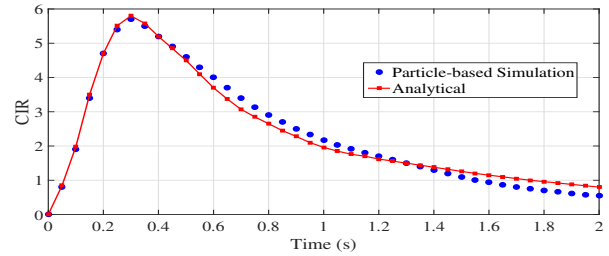

Fig. 6: Analytical and simulation results for the CIR, when $r_0 = 20\mu m$, $\varphi_1 = 0$ and $\theta = 45^o$.

However, there is no closed-form solution for (36) in the diffusion-based molecular communication systems. Fortunately, this quantity can be computed numerically. The mutual information rate can be derived as $I(X;Y) = H(Y) - H(Y|X)$. The second term, i.e., $H(Y|X)$ can be easily calculated, whereas $H(Y)$ cannot. The Shannon-McMillan-Breiman theorem states that the sample entropy rate $\hat{H}_n(Y)$ converges to the true entropy rate $H(Y)$ with probability 1 for stationary ergodic random processes [53]. Since the diffusion-based molecular communication channel is ergodic [54], we can estimate $H(Y)$ numerically by generating a long sequence of the output bits. The achievable information rate of the ergodic finite state ISI channels was studied in [53]. We use the proposed recursive calculations in [53] to derive the value of $\hat{H}_n(Y)$.

A molecular communication channel is a finite state channel which can be defined by its discrete input alphabet X, its discrete output alphabet Y, and its finite set of states Q. We use the definition $\alpha_k(q) = \Pr\left(Q_k = q | y_1^{k-1}\right)$ [53], where $y_k^{k'} = \{y_k, y_{k+1}, \ldots, y_{k'}\}$, and we have the following forward recursion:

$$\alpha_{k+1}(q) = \sum_{q' \in Q} \alpha_k(q')\, \Pr\left(Q_{k+1} = q | Q_k = q', y_k\right). \tag{37}$$

In the expression in (37), the identity $\Pr\left(Q_{k+1} | Q_k, y_1^k\right) = \Pr\left(Q_{k+1} | Q_k, y_k\right)$ is used due to the conditional independence of y_1^{k-1} and Q_{k+1} given Q_k. Finally, the entropy $\hat{H}_n(Y)$ is defined as

$$\hat{H}_{k+1}(y) = \frac{k}{k+1}\hat{H}_k(y) + \frac{1}{k+1}\Delta\hat{H}_k(y), \tag{38}$$

where $\Delta\hat{H}_{k+1}(y) = -\log \sum_{q \in Q} \alpha_{k+1}(q)\, \Pr\left(y_{k+1} | Q_{k+1} = q\right)$. Hence, the mutual information can be estimated as $I(X;Y) = \hat{H}_n(Y) - H(Y|X)$. The achievable rate per transmission provides the capacity of successfully transmission in a symbol duration. Hence, the data rate of BDSK modulation in bits per second is derived as $R = \frac{C}{T}$.

VI. Numerical Results

In this section, we present particle based simulation to appraise the performance of BDSK modulation. We clarify more

about particle based simulation in Appendix D. The numerical computations are carried out by using MatLab software.

A. Channel Impulse Response

In this section, we investigate how the concentration of molecules in the diffusion environment fluctuates through numerical results. We consider a scenario based on the presented system model in Section II. The parameters of simulated scenario are listed in Table I. We use channel impulse response (CIR) which is defined as the expected number of molecules counted at the receiver at time t after the instantaneous release of a known number of molecules by the transmitter at time $t = 0$ [55]. The CIR can be determined as

$$c(t) = \int_{V_r} \Upsilon(r, \theta, \varphi, t|R(\varphi_1), \varphi_1) dV_r, \tag{39}$$

where V_r is the receiver volume and $\Upsilon(r, \theta, \varphi, t|R(\varphi_1), \varphi_1)$ is the concentration of molecules at time t. Fig. 6 and Fig. 5 depict the CIR when the distance between the transmitter and receiver pair is $r_0 = 15\mu m$ and $r_0 = 20\mu m$, respectively. As can be observed, the simulation results justify the analytical results. The peaks of figures occur at the same time, and the values of peaks are close to each other. The CIR is increasing over time in the beginning, and then it is decreasing over time. In fact, after a period of time, i.e., $0.2 - 0.3\,s$ in the simulated scenarios, the maximum value of the concentration of molecules moves to the receiver side. It is worth mentioning that minor differences between simulation and analytical results are because of the initial velocity selection and the random acceleration selection in the simulation scenarios.

B. BDSK Modulation Analysis

In this section, we present the numerical results to analyze the performance of BDSK modulation scheme. We study the error probability and the achievable rate which are obtained in Section V, respectively. Furthermore, we investigate the impact of symbol duration, the distance between transmitter and receiver nano-machines and the value of diffusion coefficient on the error probability and achievable rate of BDSK modulation. In our analysis, the symbol duration is selected from the range $(0.2 - 6)$ ms. To evaluate the theoretical results, we simulate a scenario where the BDSK scheme is employed to transmit information according to the parameters values in Table I, when we hypothesize that $\varphi_1 = \frac{\pi}{8}$ and $\varphi_2 = -\frac{\pi}{8}$.

Fig. 7 shows the simulation and theoretical error probability of BDSK modulation versus different values of symbol duration for diverse distances between the receiver and transmitter nano-machines. First of all, the simulation and theoretical values match each other well. As can be observed, the error probability is decreased for longer symbol durations since the number of inter symbol interference molecules is reduced. Moreover, it is apparent that the error probability of BDSK modulation is increased when transmitter and receiver nano-machines are farther away due to the dispersion of molecules. Hence, we can conclude that a larger symbol duration is required for error-free communication in longer distances. Fig. 8 shows the simulation and theoretical achievable rate of BDSK modulation versus different values of symbol duration for diverse distances between the receiver and transmitter nano-machines. As can be seen, the achievable rate has a peak in a specific value of symbol duration. This value is the optimum symbol duration for designing a molecular communication system with employing BDSK modulation. In fact, achievable rate according to the expressions in Section V is a function of P_e and T. When T is reduced, the bit rate is enhanced since T is in the denominator of the bit rate. However, for symbol durations shorter than the optimum value, the bit rate is decreased since according to Fig. 7, P_e goes up. The optimum symbol duration is increased for longer distances.

Fig. 9 shows the simulation and theoretical error probability of BDSK modulation versus different values of symbol duration for diverse diffusion coefficients. It is apparent that the error probability of BDSK modulation is increased for lower values of D since the diffusion process of molecules takes more time. Hence, we can conclude that a larger symbol duration is required for error-free communication in the environments with lower diffusion coefficients. Fig. 10 depicts the achievable rate of BDSK modulation versus different values of symbol duration for diverse diffusion coefficients. Similar to Fig. 8, the achievable rate has a peak in a specific value of symbol duration. This peak is the optimum value of symbol duration for designing a molecular communication system with employing BDSK modulation. The optimum symbol duration is increased when the diffusion coefficient is reduced.

VII. Conclusion

Existing molecular communication modulation schemes encode information in terms of the concentration, type, ratio or releasing time of molecules. In this paper, we proposed the BDSK modulation scheme which used the direction of releasing molecules to convey information which reduces multi-users interference in the molecular communication relay systems in IoNT. We obtained the concentration of molecules in the 3-D diffusion environment. To the best of our knowledge, this paper is the first analytical work in the literature on the concentration of molecules when the transmitter releases molecules in a specific direction. Then, we analyzed BDSK modulation. In this modulation, we assumed that the transmitter releases molecules in two different directions and we considered a spherical receiver which is composed two sectors. We investigated the hitting probability and the number of molecules absorbed by each spherical sector and we designed an optimum receiver for BDSK modulation according to the number of absorbed molecules. Finally, we studied the error probability and achievable rate of BDSK modulation for different values of symbol duration and different distances between the receiver and transmitter nano-machines through employing theoretical and simulation results. It was observed that BDSK modulation outperforms other modulation schemes in terms of the achievable data rate. Moreover, the achievable rate of BDSK scheme had a peak in a specific value of symbol duration. The optimum value of symbol duration was increased for longer distances.

The result of this paper can be useful for multi-users interference mitigation in the new generation of molecular communication relay systems where relay nodes are located in different directions to convey information.

Appendix A
Proof of Proposition 1

Multiplying by r, the expression in (10) becomes

$$\frac{\partial \left(r\,\lambda(r, t|R(\varphi_1), \varphi_1)\right)}{\partial t} = D\,\frac{\partial^2}{\partial r^2}\left(r\,\lambda(r, t|R(\varphi_1), \varphi_1)\right), \tag{A.1}$$

where $\lambda(r, t|R(\varphi_1), \varphi_1)$ is spherically symmetric and depends on r and t. Then, we describe $\lambda(r, t|R(\varphi_1), \varphi_1)$ as the sum of

This article has been accepted for publication in IEEE Internet of Things Journal. This is the author's version which has not been fully edited and content may change prior to final publication. Citation information: DOI 10.1109/JIOT.2022.3168658

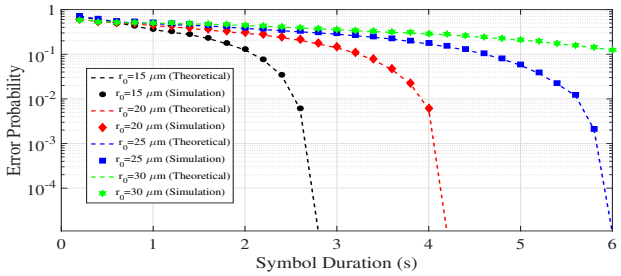

Fig. 7: Error probability of BDSK modulation versus different values of symbol duration for diverse distances between the transmitter and receiver when $D = 80\,\mu m^2$.

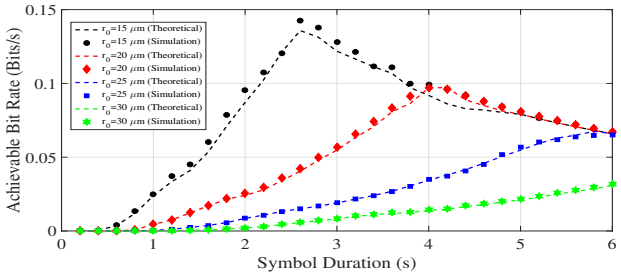

Fig. 8: Achievable rate of BDSK modulation versus different values of symbol duration for diverse distances between the transmitter and receiver when $D = 80\,\mu m^2$.

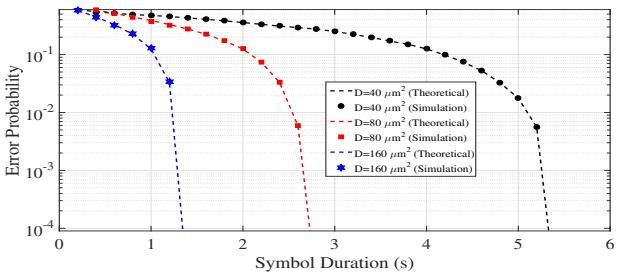

Fig. 9: Error probability of BDSK modulation versus different values of symbol duration for diverse diffusion coefficients, i.e., D, when $r_0 = 15\,\mu m$.

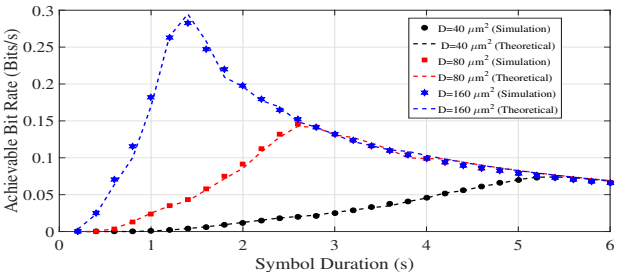

Fig. 10: Achievable rate of BDSK modulation versus different values of symbol duration for diverse diffusion coefficients, i.e., D, when $r_0 = 15\,\mu m$.

two terms, i.e., $\xi(r,t|R(\varphi_1),\varphi_1)$ and $\chi(r,t|R(\varphi_1),\varphi_1)$ as

$$\lambda(r,t|R(\varphi_1),\varphi_1) = \xi(r,t|R(\varphi_1),\varphi_1) + \chi(r,t|R(\varphi_1),\varphi_1). \tag{A.2}$$

These terms individually obey the expression in (A.1) and together obey the initial condition in (13). Thus, the function $\xi(r,t|R(\varphi_1),\varphi_1)$ is obtained by solving the following problem:

$$\frac{\partial\left(r\xi(r,t|R(\varphi_1),\varphi_1)\right)}{\partial t} = D\,\frac{\partial^2}{\partial r^2}\left(r\xi(r,t|R(\varphi_1),\varphi_1)\right), \tag{A.3}$$

with considering the initial condition

$$r\xi(r,t\to 0|R(\varphi_1),\varphi_1) = N\delta(r - R(\varphi_1)). \tag{A.4}$$

On the other hand, the function $\chi(r,t|R(\varphi_1),\varphi_1)$ should satisfy

$$\frac{\partial\left(r\chi(r,t|R(\varphi_1),\varphi_1)\right)}{\partial t} = D\,\frac{\partial^2}{\partial r^2}\left(r\chi(r,t|R(\varphi_1),\varphi_1)\right), \tag{A.5}$$

using the following initial condition $r\chi(r,t\to 0|R(\varphi_1),\varphi_1) = 0$. To solve the problem in (A.3), we partition function $\xi(r,t|R(\varphi_1),\varphi_1)$ into $\xi_1(r|R(\varphi_1),\varphi_1)$ and $\xi_2(t|R(\varphi_1),\varphi_1)$ as

$$\xi(r,t|R(\varphi_1),\varphi_1) = \xi_1(r|R(\varphi_1),\varphi_1)\xi_2(t|R(\varphi_1),\varphi_1), \tag{A.6}$$

where $\xi_1(r|R(\varphi_1),\varphi_1)$ is only a function of r and $\xi_2(t|R(\varphi_1),\varphi_1)$ is only a function of t. Inserting (A.6) into (A.3), it results

$$r\,\xi_1(r|R(\varphi_1),\varphi_1)\,\frac{\partial\xi_2(t|R(\varphi_1),\varphi_1)}{\partial t} =$$

$$D\,\xi_2(t|R(\varphi_1),\varphi_1)\,\frac{\partial^2}{\partial r^2}\left(r\,\xi_1(r|R(\varphi_1),\varphi_1)\right). \tag{A.7}$$

Dividing the expression in (A.7) by $D\,\xi_1(r|R(\varphi_1),\varphi_1)\,\xi_2(t|R(\varphi_1),\varphi_1)\,r$, we have

$$\frac{1}{D\,\xi_2(t|R(\varphi_1),\varphi_1)}\,\frac{\partial\xi_2(t|R(\varphi_1),\varphi_1)}{\partial t} =$$

$$\frac{1}{r\,\xi_1(r|R(\varphi_1),\varphi_1)}\,\frac{\partial^2}{\partial r^2}\left(r\,\xi_1(r|R(\varphi_1),\varphi_1)\right). \tag{A.8}$$

The left hand side of the expression in (A.8) is only a function of t, and the right hand side of this expression is only a function of r. Therefore, each side of this equation must be equal to a constant value. We denote this constant value as $-Dk^2$. Hence, considering the left hand side of the expression in (A.8), we obtain

$$\xi_2(t|R(\varphi_1),\varphi_1) = \exp(-Dk^2t). \tag{A.9}$$

Next, we denote the Fourier transform of $r\,\xi_1(r|R(\varphi_1),\varphi_1)$ as $\Xi_1(k|R(\varphi_1),\varphi_1)$ which satisfies

$$r\,\xi_1(r|R(\varphi_1),\varphi_1) = \frac{1}{2\pi}\int_{-\infty}^{+\infty}\Xi_1(k|R(\varphi_1),\varphi_1)e^{jkr}dk. \tag{A.10}$$

Plugging the expression in (A.10) into the right hand side of the expression in (A.8), we conclude that $\Xi_1(k|R(\varphi_1),\varphi_1) = K_\xi$, where K_ξ is a time-independent coefficient. Deriving the Fourier transform of the expression in (A.6) in respect to r and inserting (A.9) and $\Xi_1(k|R(\varphi_1),\varphi_1)$ into the resulted expression, we obtain

$$\Xi(k,t|R(\varphi_1),\varphi_1) = K_\xi\exp(-Dk^2t). \tag{A.11}$$

Note that K_ξ can be determined by using the initial condition in (A.4). When $t = 0$, we have $\Xi(k,0|R(\varphi_1),\varphi_1) = K_\xi$. The Fourier transform of the initial condition in (A.4) is given by $K_\xi = N\exp(-jkR(\varphi_1))$. Inserting K_ξ into (A.10), we obtain

$$r\xi(r,t|R(\varphi_1),\varphi_1) =$$

$$\frac{N}{2\pi}\int_{-\infty}^{+\infty}\exp(-Dtk^2)\exp\left(-jk\left(R(\varphi_1)-r\right)\right)dk. \tag{A.12}$$

The expression in (A.12) is simplified to

$$r\xi(r,t|R(\varphi_1),\varphi_1) = \frac{N}{\sqrt{4\pi Dt}}\exp\left(-\frac{\left(r-R(\varphi_1)\right)^2}{4Dt}\right). \tag{A.13}$$

This article has been accepted for publication in IEEE Internet of Things Journal. This is the author's version which has not been fully edited and content may change prior to final publication. Citation information: DOI 10.1109/JIOT.2022.3168658

Then, for solving the problem in (A.5), we employ Laplace transform. Hence, we can write

$$\frac{S}{D}\, r\, \mathrm{X}(r,S|R(\varphi_1),\varphi_1) = \frac{\partial^2}{\partial r^2}\left(r\, \mathrm{X}(r,S|R(\varphi_1),\varphi_1)\right), \quad \text{(A.14)}$$

where $\mathrm{X}(r,S|R(\varphi_1),\varphi_1)$ is the Laplace transform of $\chi(r,t|R(\varphi_1),\varphi_1)$. Solving the differential equation in (A.14) results in

$$r\, \mathrm{X}(r,S|R(\varphi_1),\varphi_1) = K_\chi \exp\left(-\sqrt{\frac{S}{D}} r\right), \quad \text{(A.15)}$$

where K_χ is a constant value and it can be calculated through the second boundary condition in (4). Considering (A.2) and employing the Laplace transform, we obtain

$$r\, \Lambda(r,S|R(\varphi_1),\varphi_1) = r\, \Xi(r,S|R(\varphi_1),\varphi_1) + r\, \mathrm{X}(r,S|R(\varphi_1),\varphi_1). \quad \text{(A.16)}$$

Moreover, the Laplace transform of $r\, \xi(r,t|R(\varphi_1),\varphi_1)$, i.e., $\Xi(r,S|R(\varphi_1),\varphi_1)$ is derived as [56]

$$\Xi(r,S|R(\varphi_1),\varphi_1) = \frac{N}{r\sqrt{4DS}} \exp\left(-\sqrt{\frac{S}{D}}\left|r - R(\varphi_1)\right|\right). \quad \text{(A.17)}$$

Inserting the expressions in (A.15) and (A.17) into (A.16), we conclude that

$$r\Lambda(r,S|R(\varphi_1),\varphi_1) = \frac{N}{r\sqrt{4DS}} \exp\left(-\sqrt{\frac{S}{D}}\left|r - R(\varphi_1)\right|\right) + K_\chi \exp\left(-\sqrt{\frac{S}{D}} r\right). \quad \text{(A.18)}$$

Due to the operator of absolute value, i.e., $|\cdot|$, in (A.18), for obtaining the value of K_χ, we divide the values of r into two domains, i.e., $r < R(\varphi_1)$ and $r \geq R(\varphi_1)$. For the first domain, i.e., $r < R(\varphi_1)$, we can write

$$r\Lambda_1(r,S|R(\varphi_1),\varphi_1) = \frac{N}{\sqrt{4DS}} \exp\left(-\sqrt{\frac{S}{D}}\left(R(\varphi_1) - r\right)\right) + K_\chi \exp\left(-\sqrt{\frac{S}{D}} r\right). \quad \text{(A.19)}$$

Using inverse Laplace transform, we obtain

$$\lambda_1(r,t|R(\varphi_1),\varphi_1) = \frac{N}{r\sqrt{4\pi Dt}} \exp\left(-\frac{\left(r - R(\varphi_1)\right)^2}{4Dt}\right) + \frac{K_\chi}{r} \exp(-\frac{r^2}{4Dt}). \quad \text{(A.20)}$$

According the second boundary condition in (4) and the expression in (A.20), we can conclude that

$$K_\chi = -\frac{N}{\sqrt{4\pi Dt}}\left[\exp\left(-\frac{R(\varphi_1)^2}{4Dt}\right) \exp\left(\frac{2r_{rx}R(\varphi_1)}{4Dt}\right)\right]. \quad \text{(A.21)}$$

Inserting the expression in (A.21) into (A.20), we derive

$$\lambda_1(r,t|R(\varphi_1),\varphi_1) = \frac{N}{r\sqrt{4\pi Dt}}[\exp\left(-\frac{\left(r - R(\varphi_1)\right)^2}{4Dt}\right) - \exp\left(-\frac{R(\varphi_1)^2}{4Dt}\right) \exp\left(\frac{2r_{rx}R(\varphi_1)}{4Dt}\right) \exp(-\frac{r^2}{4Dt})]. \quad \text{(A.22)}$$

For the second domain, i.e., $r \geq R(\varphi)$, according to (A.18) we have

$$r\Lambda_2(r,S|R(\varphi_1),\varphi_1) = \frac{N}{\sqrt{4DS}} \exp\left(-\sqrt{\frac{S}{D}}\left(r - R(\varphi_1)\right)\right) + K_\chi \exp\left(-\sqrt{\frac{S}{D}} r\right). \quad \text{(A.23)}$$

Using inverse Laplace transform, we obtain

$$\lambda_2(r,t|R(\varphi_1),\varphi_1) = \frac{N}{r\sqrt{4\pi Dt}} \exp\left(-\frac{\left(r - R(\varphi_1)\right)^2}{4Dt}\right) + \frac{K_\chi}{r} \exp(-\frac{r^2}{4Dt}). \quad \text{(A.24)}$$

According to the third boundary in (5) and the expression in (A.24), we can conclude that

$$\mathrm{K}_\chi = -\frac{N}{\sqrt{4\pi Dt}} \frac{2Dt + R(\varphi)^2 - R(\varphi)R(\varphi_1)}{R(\varphi)^2 + 2Dt} \times \exp\left(-\frac{R(\varphi_1)^2 - 2R(\varphi)R(\varphi_1)}{4Dt}\right). \quad \text{(A.25)}$$

Inserting the expression in (A.25) into (A.24), we derive

$$\lambda_2(r,t|R(\varphi_1),\varphi_1) = \frac{N}{r\sqrt{4\pi Dt}}[\exp\left(-\frac{\left(r - R(\varphi_1)\right)^2}{4Dt}\right) - \frac{2Dt + R(\varphi)^2 - R(\varphi)R(\varphi_1)}{R(\varphi)^2 + 2Dt} \times \exp\left(-\frac{R(\varphi_1)^2 - 2R(\varphi)R(\varphi_1)}{4Dt}\right) \exp(-\frac{r^2}{4Dt})]. \quad \text{(A.26)}$$

The molecules are reflected when they collide the surface of transmitter and return to the diffusion environment. Merging the expressions in (A.22) and (A.26), the concentration of molecules in the diffusion environment is derived as

$$\lambda_f(r,t|R(\varphi_1),\varphi_1) = \lambda_1(r,t|R(\varphi_1),\varphi_1) + \lambda_2(r,t|R(\varphi_1),\varphi_1). \quad \text{(A.27)}$$

Appendix B
Proof of Proposition 2

We consider the second part of the diffusion problem in (11) as

$$\frac{\partial \beta(\theta,t|R(\varphi_1),\varphi_1)}{\partial t} = \frac{D}{r^2 \sin(\theta)} \frac{\delta}{\delta\theta}\left(\sin(\theta) \frac{\delta \beta(\theta,t|R(\varphi_1),\varphi_1)}{\delta\theta}\right). \quad \text{(B.1)}$$

For solving the problem in (B.1), we partition the function $\beta(\theta,t|R(\varphi_1),\varphi_1)$ into $\beta_1(\theta|R(\varphi_1),\varphi_1)$ and $\beta_2(t|R(\varphi_1),\varphi_1)$ as

$$\beta(\theta,t|R(\varphi_1),\varphi_1) = \beta_1(\theta|R(\varphi_1),\varphi_1)\beta_2(t|R(\varphi_1),\varphi_1), \quad \text{(B.2)}$$

where $\beta_1(\theta|R(\varphi_1),\varphi_1)$ is only a function of θ and $\beta_2(t|R(\varphi_1),\varphi_1)$ is only a function of t. Plugging the expression in (B.2) into (B.1), we obtain

$$\frac{r^2 \sin(\theta)}{D} \beta_1(\theta|R(\varphi_1),\varphi_1) \frac{\partial \beta_2(t|R(\varphi_1),\varphi_1)}{\partial t} = \beta_2(t|R(\varphi_1),\varphi_1) \frac{\delta}{\delta\theta}\left(\sin(\theta) \frac{\delta \beta_1(\theta|R(\varphi_1),\varphi_1)}{\delta\theta}\right). \quad \text{(B.3)}$$

Dividing the expression in (B.2) by $\sin(\theta)\beta_1(\theta|R(\varphi_1),\varphi_1)\beta_2(t|R(\varphi_1),\varphi_1)$, we derive

$$\frac{r^2}{D} \frac{1}{\beta_2(t|R(\varphi_1),\varphi_1)} \frac{\partial \beta_2(t|R(\varphi_1),\varphi_1)}{\partial t} = \frac{1}{\sin(\theta)} \frac{1}{\beta_1(\theta|R(\varphi_1),\varphi_1)} \frac{\delta}{\delta\theta}\left(\sin(\theta) \frac{\delta \beta_1(\theta|R(\varphi_1),\varphi_1)}{\delta\theta}\right). \quad \text{(B.4)}$$

This article has been accepted for publication in IEEE Internet of Things Journal. This is the author's version which has not been fully edited and content may change prior to final publication. Citation information: DOI 10.1109/JIOT.2022.3168658

The left hand side of the expression in (B.4) is only a function of t and the right hand side is only a function of θ. Hence, each side of this equation should be equal to a constant value which is denoted by A. Thus, considering the left hand side of the expression in (B.4), we have

$$\frac{r^2}{D}\frac{1}{\beta_2(t|R(\varphi_1),\varphi_1)}\frac{\partial\beta_2(t|R(\varphi_1),\varphi_1)}{\partial t}=A, \tag{B.5}$$

and considering the right hand side of the expression in (B.4), we have

$$\frac{1}{\sin(\theta)}\frac{1}{\beta_1(\theta|R(\varphi_1),\varphi_1)}[\cos(\theta)\frac{\delta\beta_1(\theta|R(\varphi_1),\varphi_1)}{\delta\theta} + \sin(\theta)\frac{\partial^2\beta_1(\theta|R(\varphi_1),\varphi_1)}{\partial\theta^2}]=A. \tag{B.6}$$

The expression in (B.6) can be simplified as

$$\frac{\partial^2\beta_1(\theta|R(\varphi_1),\varphi_1)}{\partial\theta^2}+\cot(\theta)\frac{\partial\beta_1(\theta|R(\varphi_1),\varphi_1)}{\partial\theta}= A\beta_1(\theta|R(\varphi_1),\varphi_1). \tag{B.7}$$

The solution of the differential equation in (B.7) is obtained as

$$\beta_1(\theta|R(\varphi_1),\varphi_1)=c_1P_{\frac{1}{2}(\sqrt{1-4A}-1)}\left(\cos(\theta)\right) + c_2Q_{\frac{1}{2}(\sqrt{1-4A}-1)}\left(\cos(\theta)\right), \tag{B.8}$$

where $P_n(x)$ and $Q_n(x)$ are the first and the second kind of Legendre functions. They are defined as $P_n(x)=\frac{1}{2^n n!}\frac{d^n}{dx^n}\left(x^2-1\right)^n$, and $Q_n(x)=P_n(x)Q_0(x)+Q_{n-1}(x)$, where $Q_0(x)=\frac{1}{2}\ln\left(\frac{1+x}{1-x}\right)$. Insertion $Q_n(x)$ into (B.8), $\beta_1(\theta|R(\varphi_1),\varphi_1)$ is simplified as

$$\beta_1(\theta|R(\varphi_1),\varphi_1)=P_{\frac{1}{2}(\sqrt{1-4A}-1)}\left(\cos(\theta)\right) \times\left(c_1+c_2Q_0\left(\cos(\theta)\right)\right)+c_2Q_{\frac{1}{2}(\sqrt{1-4A}-1)-1}\left(\cos(\theta)\right). \tag{B.9}$$

In the expression in (B.9), the term $c_1+c_2Q_0\left(\cos(\theta)\right)$ is defined as

$$c_1+c_2Q_0\left(\cos(\theta)\right)=c_1+c_2\frac{1}{2}\mathrm{Ln}\frac{1+\cos(\theta)}{1-\cos(\theta)}. \tag{B.10}$$

When $\theta=0$ and $\theta=\pi$, the second term of the expression in (B.10) will be infinite. Thus, c_2 should be zero. Hence, (B.9) is simplified as

$$\beta_1(\theta|R(\varphi_1),\varphi_1)=c_1P_{\frac{1}{2}(\sqrt{1-4A}-1)}\left(\cos(\theta)\right). \tag{B.11}$$

Since the term $\beta_1(\theta|R(\varphi_1),\varphi_1)$ should be more than zero, the term $P_{\frac{1}{2}(\sqrt{1-4A}-1)}\left(\cos(\theta)\right)$ should be always positive or always negative. Therefore, we can conclude that $\sqrt{1-4A}-1=0\rightarrow A=0$, since $P_0\left(\cos(x)\right)$ is the only Legendre function which can satisfy the mention condition. Thus, the expression in (B.11) can be rewritten as $\beta_1(\theta|R(\varphi_1),\varphi_1)=c_1P_0\left(\cos(\theta)\right)$, where $P_0\left(\cos(\theta)\right)=1$, and thus, $\beta_1=c_1$. Hence, according to the expressions in (B.5) and $A=0$, we have

$$\frac{r^2}{D}\frac{1}{\beta_2(t|R(\varphi_1),\varphi_1)}\frac{\partial\beta_2(t|R(\varphi_1),\varphi_1)}{\partial t}=0, \tag{B.12}$$

and thus, we can conclude that $\frac{\partial\beta_2(t|R(\varphi_1),\varphi_1)}{\partial t}=0$. Hence $\beta_2(t|R(\varphi_1),\varphi_1)=cte$. Finally, according to the expressions $\beta_1=c_1$ and $\beta_2=cte$, we conclude that $\beta(\theta,t|R(\varphi_1),\varphi_1)=cte$. Since $\beta(\theta,t=0|R(\varphi_1),\varphi_1)=1$, we have $\beta(\theta,t|R(\varphi_1),\varphi_1)=1$.

APPENDIX C
PROOF OF PROPOSITION 3

Next, we consider the third part of the diffusion problem in (12). For solving the problem in (12) for a constant r, we define $B=\frac{D}{r^2\sin^2\theta}$, where $B\geq 0$ since $D\geq 0$. Hence, the expression in (12) is converted to

$$\frac{\partial\gamma(\varphi,t|R(\varphi_1),\varphi_1)}{\partial t}=B\frac{\partial^2}{\partial\varphi^2}\gamma(\varphi,t|R(\varphi_1),\varphi_1). \tag{C.1}$$

Moreover, we consider the initial condition in (15) for solving this problem. We define $\gamma(\varphi,t|R(\varphi_1),\varphi_1)$ as the sum of two terms, i.e., $\eta(\varphi,t|R(\varphi_1),\varphi_1)$ and $\upsilon(\varphi,t|R(\varphi_1),\varphi_1)$, as

$$\gamma(\varphi,t|R(\varphi_1),\varphi_1)=\eta(\varphi,t|R(\varphi_1),\varphi_1)+\upsilon(\varphi,t|R(\varphi_1),\varphi_1). \tag{C.2}$$

These terms individually obey the expression in (12) and together obey the initial condition in (15). Therefore, the function $\eta(\varphi,t|R(\varphi_1),\varphi_1)$ should satisfy

$$\frac{\partial\eta(\varphi,t|R(\varphi_1),\varphi_1)}{\partial t}=B\frac{\partial^2}{\partial\varphi^2}\eta(\varphi,t|R(\varphi_1),\varphi_1), \tag{C.3}$$

when we consider the initial condition

$$\eta(\varphi,t\rightarrow 0|R(\varphi_1),\varphi_1)=\delta(\varphi-\varphi_1). \tag{C.4}$$

On the other hand, the function $\upsilon(\varphi,t|R(\varphi_1),\varphi_1)$ is derived through solving the following problem:

$$\frac{\partial\upsilon(\varphi,t|R(\varphi_1),\varphi_1)}{\partial t}=B\frac{\partial^2}{\partial\varphi^2}\upsilon(\varphi,t|R(\varphi_1),\varphi_1), \tag{C.5}$$

with considering the following initial condition:

$$\upsilon(\varphi,t\rightarrow 0|R(\varphi_1),\varphi_1)=0. \tag{C.6}$$

For solving the problem in (C.3), we partition the function $\eta(\varphi,t|R(\varphi_1),\varphi_1)$ into $\eta_1(\varphi|R(\varphi_1),\varphi_1)$ and $\eta_2(t|R(\varphi_1),\varphi_1)$ as

$$\eta(\varphi,t|R(\varphi_1),\varphi_1)=\eta_1(\varphi|R(\varphi_1),\varphi_1)\,\eta_2(t|R(\varphi_1),\varphi_1), \tag{C.7}$$

where $\eta_1(\varphi|R(\varphi_1),\varphi_1)$ is only a function of φ and $\eta_2(t|R(\varphi_1),\varphi_1)$ is only a function of t. Plugging the expression in (C.7) into (C.3), we obtain

$$\eta_1(\varphi|R(\varphi_1),\varphi_1)\frac{\partial\eta_2(t|R(\varphi_1),\varphi_1)}{\partial t} = B\,\eta_2(t|R(\varphi_1),\varphi_1)\frac{\partial^2\eta_1(\varphi|R(\varphi_1),\varphi_1)}{\partial\varphi^2}. \tag{C.8}$$

Dividing the expression in (C.8) by $B\,\eta_1(\varphi|R(\varphi_1),\varphi_1)\,\eta_2(t|R(\varphi_1),\varphi_1)$, we derive

$$\frac{1}{B\,\eta_2(t|R(\varphi_1),\varphi_1)}\frac{\partial\eta_2(t|R(\varphi_1),\varphi_1)}{\partial t} = \frac{1}{\eta_1(\varphi|R(\varphi_1),\varphi_1)}\frac{\partial^2\eta_1(\varphi|R(\varphi_1),\varphi_1)}{\partial\varphi^2}. \tag{C.9}$$

For a constant r, the left hand side of the expression in (C.9) is only a function of t and the right hand side is only a function of φ. Hence, each side of this equation should be equal to a constant value which is denoted by $-Bq^2$. Thus, considering the left hand side of the expression in (C.9), we have

$$\eta_2(t|R(\varphi_1),\varphi_1)=\exp(-Bq^2t). \tag{C.10}$$

We denote the Fourier transform of $\eta_1(\varphi|R(\varphi_1),\varphi_1)$ as $\mathrm{H}_1(q|R(\varphi_1),\varphi_1)$ which satisfies

$$\eta_1(\varphi|R(\varphi_1),\varphi_1)=\frac{1}{2\pi}\int_{-\infty}^{+\infty}\mathrm{H}_1(q|R(\varphi_1),\varphi_1)\exp(jq\varphi)dq. \tag{C.11}$$

This article has been accepted for publication in IEEE Internet of Things Journal. This is the author's version which has not been fully edited and content may change prior to final publication. Citation information: DOI 10.1109/JIOT.2022.3168658

Inserting the expression in (C.11) into the right hand side of (C.9), we derive $\mathrm{H}_1(q|R(\varphi_1),\varphi_1) = K_\eta$, where K_η is a time-independent coefficient. Deriving the Fourier transform of the expression in (C.7) in respect to φ, i.e., $\mathrm{H}(q,t|R(\varphi_1),\varphi_1)$ and inserting (C.10) and $\mathrm{H}_1(q|R(\varphi_1),\varphi_1) = K_\eta$ into the resulted expression, we obtain

$$\mathrm{H}(q,t|R(\varphi_1),\varphi_1) = K_\eta \exp(-Bq^2 t). \tag{C.12}$$

Note that K_η is determined through exploiting the initial condition in (C.4). When $t = 0$, it is concluded that $\mathrm{H}(q,0|R(\varphi_1),\varphi_1) = K_\eta$. Thus, using Fourier transform of the initial condition in (C.4), we obtain $K_\eta = \exp(-jq\varphi_1)$. Using inverse Fourier transform, the expression in (C.12) is converted to

$$\eta(\varphi,t|R(\varphi_1),\varphi_1) = \frac{1}{2\pi}\int_{-\infty}^{+\infty} \exp\left(-Btq^2\right)\exp(-jq(\varphi_1-\varphi))dq. \tag{C.13}$$

After deriving the integral, the expression in (C.13) yields

$$\eta(\varphi,t|R(\varphi_1),\varphi_1) = \frac{1}{\sqrt{4\pi Bt}}\exp\left(-\frac{(\varphi-\varphi_1)^2}{4Bt}\right). \tag{C.14}$$

Next, for solving the problem in (C.5), we use Laplace transform. Hence, from (C.5), we obtain

$$\frac{S}{B}\mathrm{N}(\varphi,S|R(\varphi_1),\varphi_1) = \frac{\partial^2}{\partial r^2}\mathrm{N}(\varphi,S|R(\varphi_1),\varphi_1), \tag{C.15}$$

where $\mathrm{N}(\varphi,S|R(\varphi_1),\varphi_1)$ is the Laplace transform of $\upsilon(\varphi,t|R(\varphi_1),\varphi_1)$. Solving the differential equation in (C.15) yields

$$\mathrm{N}(\varphi,S|R(\varphi_1),\varphi_1) = K_\upsilon \exp\left(-\sqrt{\frac{S}{B}}\varphi\right), \tag{C.16}$$

where K_υ is a constant value. Deriving the Laplace transform of the expression in (C.2), we have

$$\Gamma(\varphi,S|R(\varphi_1),\varphi_1) = \mathrm{H}(\varphi,S|R(\varphi_1),\varphi_1) + \mathrm{N}(\varphi,S|R(\varphi_1),\varphi_1). \tag{C.17}$$

Furthermore, the Laplace transform of $\eta(\varphi,t|R(\varphi_1),\varphi_1)$, i.e., $\mathrm{H}(\varphi,S|R(\varphi_1),\varphi_1)$ according to (C.14) is [56]

$$\mathrm{H}(\varphi,S|R(\varphi_1),\varphi_1) = \frac{1}{\sqrt{4BS}}\exp\left(-\sqrt{\frac{S}{B}}|\varphi-\varphi_1|\right). \tag{C.18}$$

Plugging the expressions in (C.16) and (C.18) into (C.17), we derive

$$\Gamma(\varphi,S|R(\varphi_1),\varphi_1) = \frac{1}{\sqrt{4BS}}\exp(-\sqrt{\frac{S}{B}}|\varphi-\varphi_1|) + K_\upsilon \exp\left(-\sqrt{\frac{S}{B}}\varphi\right). \tag{C.19}$$

Using the inverse Laplace transform, we obtain $\gamma(\varphi,t|R(\varphi_1),\varphi_1)$ as

$$\gamma(\varphi,t|R(\varphi_1),\varphi_1) = \frac{r\sin\theta}{\sqrt{4\pi Dt}} \times \left(\exp\left(-\frac{r^2\sin^2\theta(\varphi-\varphi_1)^2}{4tD}\right) + K_\upsilon\frac{\varphi}{t}\exp\left(-\frac{r^2\sin^2\theta\varphi^2}{4tD}\right)\right). \tag{C.20}$$

According to the presented system model in Section II, the transmitter nano-machine releases molecules in the direction of $\varphi = \varphi_1$. Thus, $\gamma(\varphi,t|R(\varphi_1),\varphi_1)$ takes its maximum value when $\varphi = \varphi_1$ for different radiuses. Therefore, we conclude that

$$\frac{\partial}{\partial\varphi}\gamma(\varphi,t|R(\varphi_1),\varphi_1)|_{\varphi=\varphi_1} = 0. \tag{C.21}$$

The derivative of $\gamma(\varphi,t|R(\varphi_1),\varphi_1)$ is derived as

$$\frac{\partial}{\partial\varphi}\gamma(\varphi,t|R(\varphi_1),\varphi_1) = \frac{-1}{\sqrt{4\pi Dt}}\frac{r^3\sin^3\theta(\varphi-\varphi_1)}{2Dt}\exp\left(-\frac{r^2\sin^2\theta(\varphi-\varphi_1)^2}{4tD}\right) + \frac{r\sin\theta}{\sqrt{4\pi Dt^{\frac{3}{2}}}}K_\upsilon\exp\left(-\frac{r^2\sin^2\theta\varphi^2}{4tD}\right) - \frac{1}{\sqrt{4\pi Dt}}\frac{r^3\sin^3\theta\varphi^2}{2t^2D}K_\upsilon\exp\left(-\frac{r^2\sin^2\theta\varphi^2}{4tD}\right). \tag{C.22}$$

For satisfying the described condition in (C.21), we obtain $K_\upsilon = 0$. Inserting the value of K_υ into (C.20), this expression is simplified as (18).

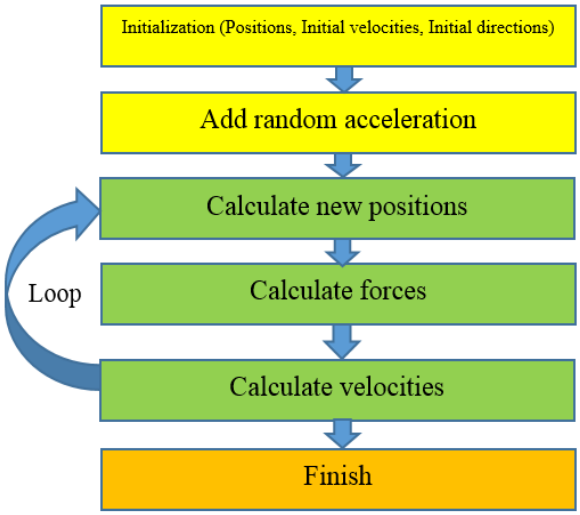

Fig. 11: Flowchart of particle based simulation process.

Appendix D
Particle Based Simulation

In this paper, we employ a classical molecular dynamic simulator which works based on Newton's equation of motion [57]. The forces between molecules are modeled as the derivatives of the potential function, where LJ Van der Waals potential is considered in this case [58]. LJ potential is a simple mathematical model of Van der Waals interactions among particles which is obtained as

$$V_{LJ} = 4\varepsilon\left[\left(\frac{\sigma}{r}\right)^{12} - \left(\frac{\sigma}{r}\right)^{6}\right], \tag{D.1}$$

where σ is the minimum distance between two molecules that there is no interaction between them. ε is the potential at the strongest attractive interaction point. Initial velocities of molecules are selected based on the pumping direction. Since the molecules have the same initial velocities, we consider a random acceleration in addition to the forces between molecules. We assume a random acceleration with a Gaussian distribution function [59].

Fig. 11 shows a flowchart of the particle based simulation process. First, the initial positions, directions and velocities of molecules are determined. Then, the simulation runs in a small

time step to predict future positions, velocities, and forces with considering the random acceleration. Thus, the velocities and positions update are obtained as

$$r_l(t+\Delta t) = r_l(t)+v_l(t)\Delta t+\frac{1}{2}\left(a_l(t)+a_l^*(t)\right)\Delta t^2, l \in \{x,y,z\} \tag{D.2}$$

$$v_l(t+\Delta t) = v_l(t) + \tfrac{1}{2}\left(a_l(t)+a_l^*(t)\right)\Delta t + \frac{1}{2}\left(a_l(t+\Delta t)+a_l^*(t+\Delta t)\right)\Delta t^2, l \in \{x,y,z\} \tag{D.3}$$

$$a_l^*(t) \sim \ N(0,{\sigma^*}^2), l \in \{x,y,z\}\,, \tag{D.4}$$

which are derived by Taylor expansion of the position and velocity at time t based on Newton's equation of motion. Moreover, $a^*(t)$ is the random acceleration.

REFERENCES

[1] K. Aghababaiyan, V. Shah-Mansouri, and B. Maham, "Direction shift keying modulation for molecular communication," *IEEE International Conference on Communications (ICC)*, Dublin, Ireland, July 2020.

[2] L. Atzori, A. Iera, and G. Morabito, "The internet of things: A survey," *Computer networks*, vol. 54, no. 15, pp. 2787–2805, Oct 2010.

[3] I. F. Akyildiz and J. M. Jornet, "The internet of nano-things," *IEEE Wireless Communications*, vol. 17, no. 6, pp. 58–63, Dec 2010.

[4] M. Kuscu and O. B. Akan, "The internet of molecular things based on FRET," *IEEE Internet of Things Journal*, vol. 3, no. 1, pp. 4–17, June 2015.

[5] T. Nakano, M. J. Moore, F. Wei, A. V. Vasilakos, and J. Shuai, "Molecular communication and networking: Opportunities and challenges," *IEEE Transactions on Nanobioscience*, vol. 11, no. 2, pp. 135–148, May 2012.

[6] I. F. Akyildiz, M. Pierobon, S. Balasubramaniam, and Y. Koucheryavy, "The internet of bio-nano things," *IEEE Communications Magazine*, vol. 53, no. 3, pp. 32–40, March 2015.

[7] W. Guo, Y. Deng, H. B. Yilmaz, N. Farsad, M. Elkashlan, A. Eckford, A. Nallanathan, and C.-B. Chae, "Smiet: Simultaneous molecular information and energy transfer," *IEEE Wireless Communications*, vol. 25, no. 1, pp. 106–113, Nov 2018.

[8] W. Guo, C. Mias, N. Farsad, and J.-L. Wu, "Molecular versus electromagnetic wave propagation loss in macro-scale environments," *IEEE Transactions on Molecular, Biological and Multi-Scale Communications*, vol. 1, no. 1, pp. 18–25, Aug 2015.

[9] W. Guo, T. Asyhari, N. Farsad, H. B. Yilmaz, B. Li, A. Eckford, and C.-B. Chae, "Molecular communications: channel model and physical layer techniques," *IEEE Wireless Communications*, vol. 23, no. 4, pp. 120–127, Aug 2016.

[10] C. Rose and I. S. Mian, "A fundamental framework for molecular communication channels: Timing & payload," *IEEE International Conference on Communications (ICC)*, London, UK, Jun 2015.

[11] N. Farsad, H. B. Yilmaz, A. Eckford, C.-B. Chae, and W. Guo, "A comprehensive survey of recent advancements in molecular communication," *IEEE Communications Surveys & Tutorials*, vol. 18, no. 3, pp. 1887–1919, Feb 2016.

[12] M. S. Kuran, H. B. Yilmaz, T. Tugcu, and I. F. Akyildiz, "Modulation techniques for communication via diffusion in nanonetworks," *IEEE International Conference on Communications (ICC)*, Kyoto, Japan, Jun 2011.

[13] N.-R. Kim and C.-B. Chae, "Novel modulation techniques using isomers as messenger molecules for nano communication networks via diffusion," *IEEE Journal on Selected Areas in Communications*, vol. 31, no. 12, pp. 847–856, Dec 2013.

[14] ——, "Novel modulation techniques using isomers as messenger molecules for molecular communication via diffusion," Ottawa, ON, Canada, June 2012.

[15] I. Llatser, A. Cabellos-Aparicio, M. Pierobon, and E. Alarcøn, "Detection techniques for diffusion-based molecular communication," *IEEE Journal on Selected Areas in Communications*, vol. 31, no. 12, pp. 726–734, Dec 2013.

[16] A. Ahmadzadeh, A. Noel, and R. Schober, "Analysis and design of multi-hop diffusion-based molecular communication networks," *IEEE Transactions on Molecular, Biological and Multi-Scale Communications*, vol. 1, no. 2, pp. 144–157, Nov 2015.

[17] H. Arjmandi, A. Gohari, M. N. Kenari, and F. Bateni, "Diffusion-based nanonetworking: A new modulation technique and performance analysis," *IEEE Communications Letters*, vol. 17, no. 4, pp. 645–648, March 2013.

[18] F. Tuerlinckx, E. Maris, R. Ratcliff, and P. De Boeck, "A comparison of four methods for simulating the diffusion process," *Behavior Research Methods, Instruments, & Computers*, vol. 33, no. 4, pp. 443–456, Nov 2001.

[19] Y. Tang, Y. Huang, C.-B. Chae, W. Duan, M. Wen, and L.-L. Yang, "Molecular type permutation shift keying in molecular MIMO communications for IoBNT," *IEEE Internet of Things Journal*, Jan 2021.

[20] T. Nakano, T. Suda, M. Moore, R. Egashira, A. Enomoto, and K. Arima, "Molecular communication for nanomachines using intercellular calcium signaling," *5th IEEE Conference on Nanotechnology*, Nagoya, Japan, Jul 2005.

[21] M. Moore, A. Enomoto, T. Nakano, R. Egashira, T. Suda, A. Kayasuga, H. Kojima, H. Sakakibara, and K. Oiwa, "A design of a molecular communication system for nanomachines using molecular motors," *Fourth Annual IEEE International Conference on Pervasive Computing and Communications Workshops (PERCOMW'06)*, Pisa, Italy, Mar 2006.

[22] Y. Moritani, S. Hiyama, and T. Suda, "Molecular communication for health care applications," *Fourth Annual IEEE International Conference on Pervasive Computing and Communications Workshops (PERCOMW'06)*, Pisa, Italy, Mar 2006.

[23] S. Hiyama, Y. Isogawa, T. Suda, Y. Moritani, and K. Sutoh, "A design of an autonomous molecule loading/transporting/unloading system using DNA hybridization and biomolecular linear motors," *arXiv preprint arXiv:0708.1839*, Aug 2007.

[24] C. Koca and O. B. Akan, "Anarchy versus cooperation on internet of molecular things," *IEEE Internet of Things Journal*, vol. 4, no. 5, pp. 1445–1453, May 2017.

[25] E. Dinc and O. B. Akan, "Theoretical limits on multiuser molecular communication in internet of nano-bio things," *IEEE transactions on nanobioscience*, vol. 16, no. 4, pp. 266–270, April 2017.

[26] X. Chen, M. Wen, C.-B. Chae, L.-L. Yang, F. Ji, and K. K. Igorevich, "Resource allocation for multi-user molecular communication systems oriented to the internet of medical things," *IEEE Internet of Things Journal*, Jan 2021.

[27] A. W. Eckford, "Molecular communication: Physically realistic models and achievable information rates," *arXiv preprint arXiv:0812.1554*, Dec 2008.

[28] S. Kadloor, R. S. Adve, and A. W. Eckford, "Molecular communication using Brownian motion with drift," *IEEE Transactions on NanoBioscience*, vol. 11, no. 2, pp. 89–99, Mar 2012.

[29] J. Wang, M. Peng, Y. Liu, X. Liu, and M. Daneshmand, "Performance analysis of signal detection for amplify-and-forward relay in diffusion-based molecular communication systems," *IEEE Internet of Things Journal*, vol. 7, no. 2, pp. 1401–1412, Nov 2019.

[30] X. Bao, Q. Shen, Y. Zhu, and W. Zhang, "Relative localization for silent absorbing target in diffusive molecular communication system," *IEEE Internet of Things Journal*, Aug 2021.

[31] M. J. Moore, T. Suda, and K. Oiwa, "Molecular communication: Modeling noise effects on information rate," *IEEE Transactions on Nanobioscience*, vol. 8, no. 2, pp. 169–180, Jun 2009.

[32] B. Atakan and O. B. Akan, "An information theoretical approach for molecular communication," *2nd Bio-Inspired Models of Network, Information and Computing Systems*, Budapest, Hungary, Dec 2007.

[33] J. Wang, X. Liu, M. Peng, and M. Daneshmand, "Performance analysis of D-MoSK modulation in mobile diffusive-drift molecular communications," *IEEE Internet of Things Journal*, vol. 7, no. 11, pp. 11 318–11 326, May 2020.

[34] P. J. Thomas, D. J. Spencer, S. K. Hampton, P. Park, and J. P. Zurkus, "The diffusion-limited biochemical signal-relay channel," *Advances in Neural Information Processing Systems*, pp. 1263–1270, 2004.

[35] B. Atakan and O. B. Akan, "Single and multiple-access channel capacity in molecular nanonetworks," *International Conference on Nano-Networks*, Oct 2009.

[36] A. P. Shrestha, S.-J. Yoo, H. J. Choi, and K. S. Kwak, "Enhanced rate division multiple access for electromagnetic nanonetworks," *IEEE Sensors Journal*, vol. 16, no. 19, pp. 7287–7296, Aug 2016.

[37] M. Kuscu, E. Dinc, B. A. Bilgin, H. Ramezani, and O. B. Akan, "Transmitter and receiver architectures for molecular communications: A survey on physical design with modulation, coding, and detection techniques," *Proceedings of the IEEE*, vol. 107, no. 7, pp. 1302–1341, 2019.

[38] J. Suzuki, T. Nakano, and M. J. Moore, "Modeling, methodologies and tools for molecular and nano-scale communications: modeling, methodologies and tools," vol. 9, 2017.

[39] M. Femminella, G. Reali, and A. V. Vasilakos, "A molecular communications model for drug delivery," *IEEE transactions on nanobioscience*, vol. 14, no. 8, pp. 935–945, Oct 2015.

[40] A. Ahmadzadeh, H. Arjmandi, A. Burkovski, and R. Schober, "Comprehensive reactive receiver modeling for diffusive molecular communication systems: Reversible binding, molecule degradation, and finite number of receptors," *IEEE transactions on nanobioscience*, vol. 15, no. 7, pp. 713–727, Sep 2016.

[41] H. B. Yilmaz, C. Lee, Y. J. Cho, and C.-B. Chae, "A machine learning approach to model the received signal in molecular communications," pp. 1–5, Istanbul, Turkey, Jun 2017.

[42] B. C. Akdeniz, N. A. Turgut, H. B. Yilmaz, C.-B. Chae, T. Tugcu, and A. E. Pusane, "Molecular signal modeling of a partially counting absorbing spherical receiver," *IEEE Transactions on Communications*, vol. 66, no. 12, pp. 6237–6246, 2018.

[43] A. Noel, Y. Deng, D. Makrakis, and A. Hafid, "Active versus passive: Receiver model transforms for diffusive molecular communication," Washington, DC, USA, Dec 2016.

This article has been accepted for publication in IEEE Internet of Things Journal. This is the author's version which has not been fully edited and content may change prior to final publication. Citation information: DOI 10.1109/JIOT.2022.3168658

[44] H. B. Yilmaz and C.-B. Chae, "Simulation study of molecular communication systems with an absorbing receiver: Modulation and ISI mitigation techniques," *Simulation Modelling Practice and Theory*, vol. 49, pp. 136–150, Dec 2014.
[45] H. C. Berg, *Random walks in biology*. Princeton University Press, Sep 1993.
[46] B. Alberts, D. Bray, K. Hopkin, A. D. Johnson, J. Lewis, M. Raff, K. Roberts, and P. Walter, *Essential cell biology*. Garland Science, 2015.
[47] K. Aghababaiyan, V. Shah-Mansouri, and B. Maham, "Capacity and error probability analysis of neuro-spike communication exploiting temporal modulation," *IEEE Transactions on Communications*, vol. 68, no. 4, pp. 2078–2089, Dec 2019.
[48] ——, "Joint optimization of input spike rate and receiver decision threshold to maximize achievable bit rate of neuro-spike communication channel," *IEEE transactions on nanobioscience*, vol. 18, no. 2, pp. 117–127, 2018.
[49] ——, "Asynchronous neuro-spike array-based communication," *IEEE International Black Sea Conference on Communications and Networking (BlackSeaCom)*, Batumi, Georgia, Aug 2018.
[50] H. B. Yilmaz, A. C. Heren, T. Tugcu, and C.-B. Chae, "Three-dimensional channel characteristics for molecular communications with an absorbing receiver," *IEEE Communications Letters*, vol. 18, no. 6, pp. 929–932, May 2014.
[51] F. Dinç, B. C. Akdeniz, A. E. Pusane, and T. Tugcu, "Impulse response of the molecular diffusion channel with a spherical absorbing receiver and a spherical reflective boundary," *IEEE Transactions on Molecular, Biological and Multi-Scale Communications*, vol. 4, no. 2, pp. 118–122, Jun 2018.
[52] L.-S. Meng, P.-C. Yeh, K.-C. Chen, and I. F. Akyildiz, "On receiver design for diffusion-based molecular communication," *IEEE Transactions on Signal Processing*, vol. 62, no. 22, pp. 6032–6044, Sep 2014.
[53] H. D. Pfister, J. B. Soriaga, and P. H. Siegel, "On the achievable information rates of finite state isi channels," San Antonio, TX, USA, Nov 2001.
[54] Y.-P. Hsieh and P.-C. Yeh, "Mathematical foundations for information theory in diffusion-based molecular communications," *arXiv preprint arXiv:1311.4431*, 2013.
[55] V. Jamali, A. Ahmadzadeh, C. Jardin, H. Sticht, and R. Schober, "Channel estimation for diffusive molecular communications," *IEEE Transactions on Communications*, vol. 64, no. 10, pp. 4238–4252, Aug 2016.
[56] D. V. Widder, *Laplace transform (PMS-6)*. Princeton university press, Dec 2015.
[57] D. Frenkel and B. Smit, *Understanding molecular simulation: from algorithms to applications*. Elsevier, 2001, vol. 1.
[58] J. E. Jones, "On the determination of molecular fields.—ii. from the equation of state of a gas," *Proceedings of the Royal Society of London. Series A, Containing Papers of a Mathematical and Physical Character*, vol. 106, no. 738, pp. 463–477, Oct 1924.
[59] Y. Miao, V. A. Feher, and J. A. McCammon, "Gaussian accelerated molecular dynamics: Unconstrained enhanced sampling and free energy calculation," *Journal of chemical theory and computation*, vol. 11, no. 8, pp. 3584–3595, Aug 2015.

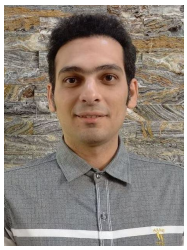

Keyvan Aghababaiyan received his B.Sc. degree in communication Engineering from Amirkabir University of Technology of Tehran, Iran in 2011 (with highest honors) and received his M.Sc. degree in Communication Engineering from Sharif University of Technology of Tehran, Iran in 2013, and received the Ph.D. degree from the University of Tehran, Tehran, Iran in 2019. His research interests include Internet of Things (IoT), Nano-neural communication systems, wireless communication and networking.

Hamed Kebriaei (SM18) was born in 1983. He received his Ph.D. degree in control systems from the University of Tehran, Iran, in 2010. He is currently an Associate Professor of Control Systems with the School of Electrical and Computer Engineering, University of Tehran, Iran. He has been the head of Control department at School of ECE, University of Tehran since 2017. He is a Senior member of IEEE, a technical committee member of IEEE CSS in Networks and Communication Systems, and a Board member of Control Systems Chapter- IEEE Iran Section. He has coauthored more than 70 research publications in reputed journals and conferences. His research interests include, Game Theory, Distributed Optimization and Multi agent learning with applications in network systems.

Vahid Shah-Mansouri (Member, IEEE) received the B.Sc. degree in electrical engineering from the University of Tehran, Tehran, Iran, in 2003, the M.Sc. degree in electrical engineering from the Sharif University of Technology, Tehran, in 2005, and the Ph.D. degree from the University of British Columbia, Vancouver, BC, Canada, in 2011. Since 2013, he has been a Faculty member at the School of Electrical and Computer Engineering, University of Tehran. His research interests include analysis and mathematical modeling of communication and computer networks and next-generation cellular systems.

Behrouz Maham (S'07, M'10. SM'15) received the B.Sc. and M.Sc. degrees in electrical engineering from the University of Tehran, Iran, in 2005 and 2007, respectively, and the Ph.D. degree from the University of Oslo, Norway, in 2010. From September 2008 to August 2009, he was with the Department of Electrical Engineering, Stanford University, Stanford, CA, USA. He is currently an Associate Professor of the ECE Department, School of Engineering, Nazarbayev University (NU). He was an Assistant Professor with the School of Electrical and Computer Engineering, University of Tehran, from Sep. 2011 to Sep. 2015. Dr. Maham is TWAS-affiliate, a Senior Member of IEEE, and has around 160 publications in major technical journals and conferences. He has been an editorial member of IEEE Transactions on Communications, Elsevier's Physical Communication, and John Wiley & Sons Transactions on Emerging Telecommunications Technologies. His fields of interest include wireless communication and networking and nano-neural communication systems.

Dusit Niyato (M'09-SM'15-F'17) is a professor in the School of Computer Science and Engineering, at Nanyang Technological University, Singapore. He received B.Eng. from King Mongkuts Institute of Technology Ladkrabang (KMITL), Thailand in 1999 and Ph.D. in Electrical and Computer Engineering from the University of Manitoba, Canada in 2008. His research interests are in the areas of Internet of Things (IoT), machine learning, and incentive mechanism design.